Original Contribution

Kurume Medical Journal, 58, 41-46, 2011

Clinicopathological Study on Poorly Differentiated Adenocarcinoma of the Colon

TAKEFUMI YOSHIDA, YOSHITO AKAGI, TETSUSHI KINUGASA, ICHITARO SHIRATSUCHI, YASUHIKO RYU AND KAZUO SHIROUZU

Department of Surgery, Kurume University School of Medicine, Kurume 830-0011, Japan

Received 6 January 2011, accepted 15 March 2011

Edited by HIROHISA YANO

Summary: Clinicopathological characteristics and grading of poorly differentiated colon adenocarcinoma (Por) were discussed. A total of 1074 patients with colon cancer underwent surgical treatment at Kurume University Hospital in Fukuoka, between 1985 and 2005. Clinicopathological characteristics of 88 cases (8%) of Por and 986 cases (92%) of well differentiated tubular adenocarcinoma/moderately differentiated tubular adenocarcinoma (Tub1/Tub2) were studied. A multiple classification analysis showed that Por was more frequently observed in the right colon than Tub1/Tub2, and that the ratio of macroscopic types 3 and 4 was significantly higher in Por. Significant differences were also observed with regard to lymph vessel and perineural invasion. There were no significant differences between recurrence-free survivals of Por and Tub1/Tub2 after radical resection in Stages Ⅱ and Ⅲ. Recurrence of Por was significantly higher in peritonea and lymph nodes. These findings indicate that Por, which is generally considered to have a poor prognosis, has a similar recurrence rate to that of Tub1/Tub2 after the performance of radical surgery.

Key words poorly differentiated colon adenocarcinoma, prognosis, perineural invasion

INTRODUCTION

Most colon cancers are classified as either well differentiated tubular adenocarcinoma (Tub1) or moderately differentiated tubular adenocarcinoma (Tub2). According to a nationwide study by Yasutomi [1], the prevalence of poorly differentiated adenocarcinoma (Por) in Japan is 4.8%. Other reports have stated it to be 2.7% to 10% in this country [2-16], while it is estimated to be approximately 20% in Europe and the United States [17,18]. There has been little discussion of the clinicopathological characteristics of Por, which is considered to have a poor prognosis. We found the prevalence of Por to be 8%, which was slightly higher than that in Yasutomi's report. The present study compared the prognosis and clinicopathological characteristics of Por with those of Tub1/Tub2. This comparison revealed abundant and significant statistical differences, which are discussed with reference to the literature.

SUBJECTS AND METHODS

A total of 1074 patients with colon cancer underwent surgical treatment at Kurume University Hospital in Fukuoka, between 1985 and 2005. All cases were associated with sporadic colon cancer. Informed consent was obtained from all patients before surgical resection was performed, and this study was approved by the Institutional Review Committee for Research on Human Subjects in Kurume University Hospital. In our department excised samples were completely segmented and the detailed characteristics of each cancer were depicted. Tumor differentiation, the degree of invasion, venous invasion, lymph vessel invasion and perineural invasion were examined by pathologists

Corresponding Author: Takefumi Yoshida M.D, 67 Asahi-machi, Kurume 830-0011, Japan. Tel: +81-942-35-3311 Fax: +81-942-34-0709 E-mail: yoshida_takefumi@med.kurume-u.ac.jp

Abbreviations: Cur A, Curability A; EVG, Elastica van Gieson; Por, poorly differentiated colon adenocarcinoma.

TABLE 1.
Data on all registered patients

Variable	Patients (n=1074)
Median age (range), years	66 (17-91)
Sex	
Female	439 (41%)
Male	635 (59%)
Tumor differentiation	
Tub1,Tub2	986 (92%)
Por	88 (8%)
Stage	
0	75 (7%)
I	180 (17%)
Ⅱ	300 (28%)
Ⅲ	304 (28%)
Ⅳ	210 (20%)
Location	
Vermiform processus	4 (<1%)
Cecum	81 (8%)
Ascending colon	179 (16%)
Transverse colon	129 (12%)
Descending colon	60 (5%)
Sigmoid colon	406 (39%)
Rectosigmoid	215 (20%)

Tub1,2: Well and moderately differentiated tubular adonocarcinoma, Por: Poorly differentiated adonocarcinoma.

and histopathological classifications were performed according to the General Rules for Clinical and Pathological Studies on Cancer of the Colon, Rectum, and Anus published by the Japanese Society for Cancer of the Colon and Rectum [19]. Venous invasion was evaluated by Elastica van Gieson (EVG) stain. Adenocarcinoma tissues were classified as Por or Tub1/Tub2 in accordance with the dominant tissue images. The subjects in this study were patients suffering recurrence or survival according to our department database. The cases were classified as either Tub1/Tub2 or Por, and the clinicopathological characteristics of each adenocarcinoma were studied. The prevalence of Por was 8% (88/1074 cases). The statistical significance of differences between Tub1/Tub2 and Por were examined using the chi-square test, Fisher's exact test, and the t-test. Cumulative survival rate was calculated using the Kaplan-Meier method with comparisons performed using the log-rank test. A logistical analysis and the Cox proportional hazard model were used for a multiple classification analysis. A p value of $<.05$ was considered significant. For statistical analysis, JMP 8 version 8.0 (SAS Institute Inc., USA) was used.

RESULTS

Clinicopathological characteristics (Table 2)

The average age of subjects with Por was 63 years, and males tended to be more susceptible as compared with Tub1/Tub2; however, these differences were not significant. No cases of Stage 0 or I Por were found. Fisher's exact test demonstrated significant differences ($p<.001$) in the following categories: stage ($p<.001$), location ($p<.001$), macroscopic type ($p<.001$), tumor size ($p<.001$), invasion depth ($p<.001$), lymph node metastasis ($p < .001$), lymph vessel invasion ($p<.001$), venous invasion ($p<.001$), and perineural invasion ($p<.001$). Logistic regression analysis extracted the following 4 items as independent factors for Por: location (right colon) ($p<.001$, confidence interval [CI]: -0.764 - -0.275, odds ratio [OR]: 2.812), macroscopic type (types 3 and 4) ($p<.001$, CI: -0.780 - -0.238, OR: 2.779), lymph vessel invasion (positive) ($p<.001$, CI: -1.397 - -0.390, OR: 5.376), and perineural invasion (positive) ($p=.032$, CI: -0.570 - -0.022, OR: 1.818). There were no significant differences in preoperative carcinoembryonic antigen (CEA) values.

Recurrence-free survival rate

Figures 1 and 2 show recurrence-free survival rates in cases where radical surgery was performed (CurabilityA (CurA)) .

In Stage Ⅱ, 14 Por and 280 Tub1/Tub2 cases were observed. Postoperative chemotherapy was given to 3 Por cases (21%) and 107 Tub1/Tub2 cases (38%). The recurrence-free survival rate of Por was lower than that of Tub1/Tub2; however, the difference was not significant (log-rank $p=.354$).

In Stage Ⅲ, 36 Por and 255 Tub1/Tub2 cases were observed. Postoperative chemotherapy was given to 14 Por cases (39%) and 122 Tub1/Tub2 cases (48%). As in Stage Ⅱ, the recurrence-free survival rate of Por was lower than that of Tub1/Tub2; however, the difference was not significant (log-rank $p=.354$).

Similarly, no significant differences in the recurrence-free survival rate were observed in Stage Ⅳ.

First recurrent pattern (Table 3)

Fisher's exact test showed significant differences in peritonea ($p=.018$) and lymph nodes ($p<.001$) in

TABLE 2.
Clinicopathological features of histological types

Variable	Tub1,Tub2	Por	χ^2	Odds ratio	CI	Multivariate analysis p value	Univariate analysis p value
Mean age±SD (y)	65±11	63±12	–	–	–	–	0.127
Sex F/M	401/585	38/50	–	–	–	–	0.652
Stage							
Ⅲ, Ⅳ/0,Ⅰ,Ⅱ	441/540	73/15	0.10	1.288	–0.840 - 0.840	0.756	<.001
Location							
V,C,A,T/D,S,Rs	342/644	51/37	17.27	2.812	–0.764 - –0.275	<.001	<.001
Macroscopic type							
3,4/1,2	99/881	31/56	13.73	2.779	–0.780 - –0.238	<.001	<.001
Tumor size (cm)							
4.5≦/4.5>	509/463	62/25	0.01	0.974	–0.274 - 0.289	0.926	<.001
Primary tumor							
si,se,ss/mp,sm,m	707/278	85/2	2.05	3.158	−1.531 - 0.118	0.152	<.001
Lymph node metastasis							
+/–	403/555	70/17	0.54	1.766	–1.221 - 0.372	0.462	<.001
Lymph vessel invasion							
+/–	537/444	82/5	11.11	5.376	–1.397 - –0.390	<.001	<.001
Venous invasion							
+/–	673/309	80/7	0.00	0.999	–0.531 - 0.457	0.998	<.001
Perineural invasion							
+/–	110/842	30/55	4.59	1.818	–0.570 - –0.022	0.032	<.001
CEA (ng/ml)							
5≦/5>	299/536	31/44	–	–	–	–	0.380

Tub1,2: Well and moderately differentiated tubular adonocarcinoma, Por: Poorly differentiated adonocarcinoma.

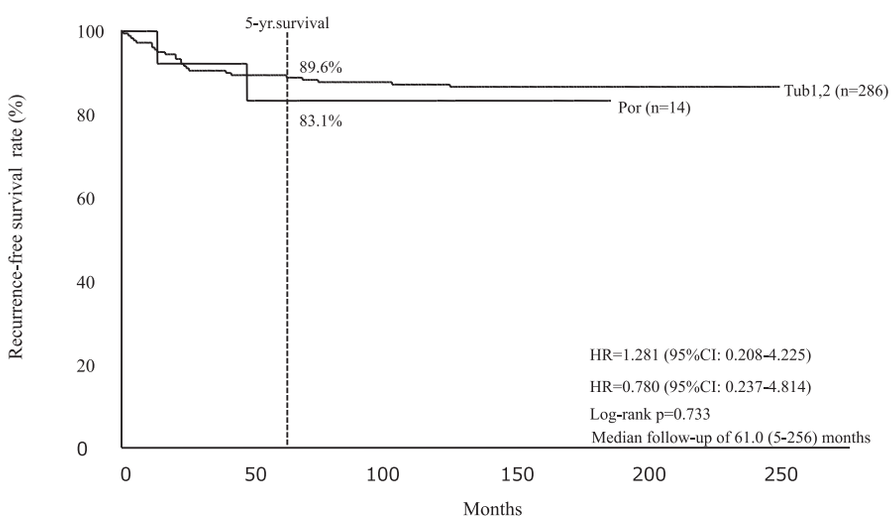

Fig. 1. Recurrence-free survival rate for patients in stage Ⅱ.
Tub1: Well differentiated type, Tub2: Moderately type, Por: Poorly differentiated adenocarcinoma.

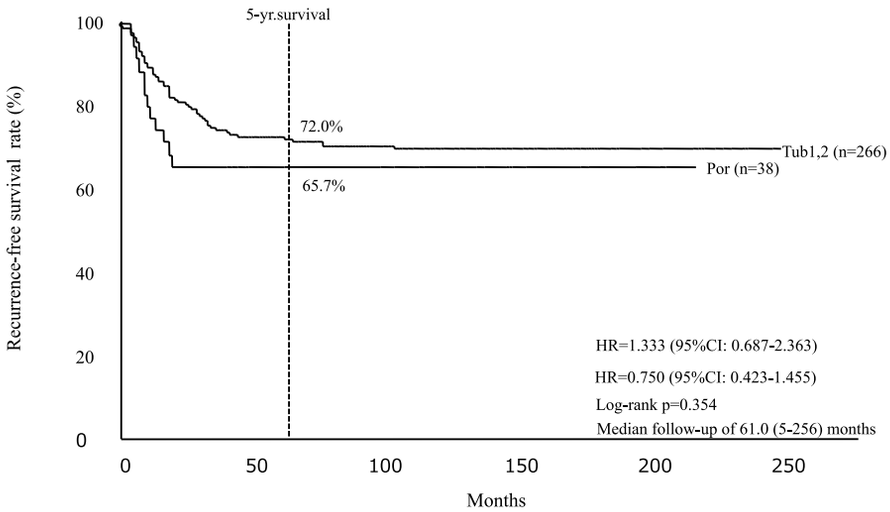

Fig. 2. Recurrence-free survival rate for patients in stage Ⅲ.
Tub1: Well differentiated type, Tub2: Moderately type, Por: Poorly differentiated adenocarcinoma.

TABLE 3.
Location of first recurrence site for patients who underwent curative operations

Factor	Tub1,Tub2 (n)	Por (n)	χ^2	Odds ratio	CI	Multivariate analysis p value	Univariate analysis p value
Liver	57	5	0.07	1.252	–0.974-0.707	0.790	0.400
Lung	33	3	0.01	0.913	–0.794-0.972	0.918	0.756
Peritoneum	16	6	6.54	9.475	–2.058-–0.298	0.011	0.018
Lymph node	7	5	9.09	20.408	–2.597-–0.560	0.003	<.001
Local	11	1	0.44	0.459	–0.608-1.906	0.505	1.000
Unknown	11	1	0.47	2.631	–1.825-1.168	0.495	1.000

*Including duplications
Tub1,2: Well and moderately differentiated tubular adonocarcinoma, Por: Poorly differentiated adonocarcinoma.

comparisons of first recurrence patterns. When lymph nodes and peritonea were subjected to logistic regression analysis, peritonea (p=.011, CI: −2.058 - −0.298, OR: 9.475) and lymph nodes (p=.003, CI: −2.597 - −0.560, OR: 20.408) were extracted as independent factors. The recurrence locations overlapped.

DISCUSSION AND CONCLUSIONS

Patients who underwent surgery for Por were younger than those with Tub1/Tub2 [20,21]. Differences in gender vary depending on the report. In our case, no significant statistical differences were found with regard to median age or gender. The clinicopathological characteristics of Por reported so far are as follows: (1) Por frequently occurs in the right colon [3-16,22]. (2) Macroscopic types 3 and 4 are frequently observed [3,4,6,7,10]. (3) Cancer invasion is deep and infiltrative [3-5,7-15]. (4) Por metastasizes at high rates [3-5,7-9,11-16]. (5) Lymph vessel and venous invasion are severe [5,7-15]. (6) The ratio of peritoneal dissemination is high [4,8,9,11-13,15,16]. (7) Clinicopathological staging is advanced [4,7-9,11-15]. (8) Prognosis is poor [3-5,7-16].

Tumor locations were concentrated in the right colon in our multiple classification analysis. Shimizu et al. [22] reported animal carcinogenesis experiments in which Por occurred in the cecum and proximal colon,

and Tub1 occurred in the distal colon. A report of hereditary nonpolyposis colorectal cancer showed that bowel cancer with microsatellite instability caused by DNA replication error had Por in the right colon [23,24]. These reports suggest a need for a study of the microsatellite instability in our case. Macroscopic types 3 and 4 were frequently observed in our multiple classification analysis, as in previous reports. For cancer invasion depth, 2 of 87 Por cases were mp, while 85 of 87 cases were se and si. The depth was greater than that of Tub1/Tub2. Statistically, there were no significant differences in the multiple classification analysis. In Por, multiple classification analysis showed significantly higher rates of lymph vessel and perineural invasion. First recurrence patterns showed significantly higher rates of Por in the peritonea and lymph nodes. Positive lymph nodes and deeper invasion implied that Por included more advanced cases with Stage Ⅲ or higher disease compared with Tub1/Tub2. The recurrence-free 5-year survival rate of Cur A cases was discussed as to prognosis. In Stage Ⅱ, the prevalence of Por was 83.1% and that of Tub1/Tub2 was 89.6%; the difference was not significant. The recurrence-free 5-year survival rate in Stage Ⅲ was 65.7% for Por and 72.0% for Tub1/Tub2; again the difference was not significant. Some studies have reported that the prognosis of Por was poorer than that of Tub1/Tub2, even after radical surgery [3-5,7-16]. To compare prognoses according to tissue type, a wider study is necessary.

In the present study, no significant difference was observed between the prognoses of Por and Tub1/Tub2 when radical surgery was performed. In the treatment guidelines for colon cancer [25], Por is defined as a Stage Ⅱ colon cancer with a high risk of recurrence. No significant differences were observed in the prognosis of Por when compared with the prognosis of Tub1/Tub2. Hence, our findings suggest that postoperative adjunctive chemotherapy may not be necessary in cases where radical surgery is provided, even in cases that are determined to be Por. However, the number of cases studied was small, and further prospective studies in multiple facilities are necessary.

A summary of this study was delivered at the 34th Annual Meeting of The Japanese Society of Coloproctology in Kyushu, Japan.

REFERENCES

1. Yasutomi Masayuki, Taiji Matsuda, Jinichi Hida et al. Colon Cancer Classification Regulaions and Epidemiology. Nichirin 1988; 46:356-356.
2. Teruyuki Hirota, Toshio Okada, Masayuki Itabashi, Yoshihiro Moriya, Yasuo Ogawa et al. Colon Cancer Tissue Type and Prognosis. Nichirin 1981; 39:2108-2116.
3. Masahiro Okuno, Teruyuki Ikehara, Masayoshi Nagayama, Yasuyuki Kato, Masaichi Ohira et al. Cinicopathological Discussion on Colon Poorly-Differentiated Adenocarcinoma. Journal of Japanese Society for Clinical Surgery 1989; 50:1307-1312.
4. Masahiro Kanno, Hiroya Sakamoto, Yuji Tsukioka, Yasushi Takano, Yoshiyuki Kurosaka et al. Cinicopathological Study on Colon Poorly-Differentiated Adenocarcinoma. Journal of Japan Society of Coloproctology 1992; 45:244-247.
5. Wataru Fukushima, Takashi Kobayashi, Hiroyuki Sahara, Hisashi Matsumoto, Naotaka Kadoya et al. Discussion on Colon Poorly-Differentiated Adenocarcinoma Cases. The Japanese Journal of Gastroenterological Surgery 1993; 26:1013-1017.
6. Masahiko Otsuka, and Yo Kato. Clinicopathological Study of Poorly Differentiated and Undifferentiated Carcinoma of the Large Intestine: Classification and Special Reference to the Endocrine Cell Carcinoma. The Japanese Journal of Gastroenterological Surgery 1992; 25:1248-1256.
7. Eiji Miyahara, Koji Ikejiri, Soichiro Maekawa, Yasuhiro Yoshida, Shigeru Yakabe et al. A Clinicopathological Studies on 25 Patients with Poorly Differentiated Adenocarcinoma of the Colon and Rectum. The Japanese Journal of Gastroenterological Surgery 1992; 25:1984-1988.
8. Takeshi Sekine, and Shinichi Kakinuma. Clinicopathological Discussion on Colon Poorly-Differentiated Adenocarcinoma. Japanese Journal of Cancer Clinics 1993; 39:485-490.
9. Yuji Inoue, Mamoru Suzuki, and Ken Takasaki. Clinicopathological Discussion on Colon Poorly-Differentiated Adenocarcinoma. Ringai 1998; 53:365-368.
10. Kazuhito Misawa, Yuji Sato, Hiroshi Saji, Masato Nakayama, Junichi Uchino et al. Clinicopathological Discussion on Colon Poorly-Differentiated Adenocarcinoma mucinous cancer: As contrasted with differentiated adenocarcinoma. Journal of Japanese Society for Clinical Surgery 1992; 53:309-312.
11. Masato Kiriyama, Yoshiyuki Kurosaka, Masahiro Matsushita, Fujio Tomita, Hitoshi Saito et al. Clinicopathological Discussion on Colon Poorly-Differentiated Adenocarcinoma. Digestive Organ Cancer 1996; 6:37-41.
12. Masahiko Ohata, Isamu Koyama, Takashi Matsumoto, Nobuko Fujiuchi, Nobuji Ogawa et al. Discussion on Colon Poorly-Differentiated Adenocarcinoma. Journal of Japanese College of Surgeons 1997; 22:878-885.
13. Harunobu Sato, Morita Maruto, Kotaro Maeda, Toshiaki Utsumi, Kunihiro Tohyama et al. Clinicopathological Discussion on Colon Poorly-Differentiated Adenocarcinoma. Journal of Japan Surgical Association 1998; 59:1214-1221.
14. Sengai Tanaka, Hiroo Oshita, and Daizo Fukada. Clinicopathological Discussion on Colon Poorly-Differentiated Adenocarcinoma. Journal of Japanese Society for Clinical Surgery 1992; 53:313-317.
15. Masakazu Ikenaga, Nobuteru Yoshikawa, Hideyuki Mishima, Isamu Nishisyo, and Toshio Yagyu. Discussion on 76 Cases of Colon Poorly-Differentiated Adenocarcinoma. Journal of Japan Society of Coloproctology 1997; 50:469-475.

16. Keiichi Kanno, Susumu Ohwada, and Yasuo Morishita. Discussion on Colon Poorly-Differentiated Adenocarcinoma and Adenocarcinoma Mucocellulare. Journal of Japanese Society for Clinical Surgery 1995; 56:1806-1810.
17. Dukes CE, and Bussey HJR. The spread of rectal cancer and its effect on prognosis. Br J Cancer 1958; 12:309-320.
18. Chung CK, Zaino RJ, and Stryker JA. Colorectal carcinoma : Evaluation of histologic grade and factors influencing prognosis. J Surg Oncol 1982; 21:143-148.
19. Yutaka Shimizu, and Saburo Nakazawa. Impacts of Dietary Factors and Bile Acid in Faces on Occurrence of DMH Induced Rat Colon Cancer. Journal of Japanese Society of Gastroenterology 1985; 82:2554-2561.
20. Scarpa FJ, Hartmann WH, and Sawyers JL. Adenocarcinoma of the colon and rectum in young adults. South Med J 1976; 69:24-27.
21. Martin EW, Joyce S, Lucas J, Clausen K, Cooperman M. Colorectal carcinoma in patients less than 40 years of age: Pathology and prognosis. Dis Colon Rectum 1981; 24:25-28.
22. Japanese Society for Cancer of the Colon and Rectum: JSCCR Guidelines 2009 for the Treatment of Colorectal Cancer. KANEHARA & CO;, LTD., Tokyo, 2009, p50-51.
23. Thibodeau SN, and Schaid BD: Microsatellite instability in cancer of the proximal colon. Science 1993; 260:816-819.
24. Lothe RA, Peltomaki P, Meling GI, Aaltonen LA, Hystrom-Lahti M et al. Genomic instability in colorectal cancer: Relationship to clinicopathological variable and family history. Cancer Res 1993; 53:5849-5852.
25. Japanese Society for Cancer of the Colon and Rectum (JSCCR): General Rules for Clinical and Pathological Studies on Cancer of the Colon, Rectum and Anus. The 7th Edition, Revised Version. Tokyo, Japan: Kanehara Shuppan, 2009.

Original Contribution

Kurume Medical Journal, 58, 47-58, 2011

Edaravone Attenuates Impairment of Synaptic Plasticity in Granule Cell Layer of the Dentate Gyrus Following Traumatic Brain Injury

SHIN YAMASHITA*,**, HIROSHI HASUO*, TAKASHI TOKUTOMI**, MINORU SHIGEMORI** AND TAKASHI AKASU*,†

Department of Physiology and Neurosurgery**, Kurume University School of Medicine, and †Cognitive and Molecular Research Institute of Brain Diseases, Open Research Center, Kurume University, Kurume 830-0011, Japan*

Received 28 December 2010, accepted 7 April 2011

Summary: Effects of edaravone, a free radical scavenger, on post-traumatic impairment of long-term potentiation (LTP) were examined in granule cell layers of the dentate gyrus (DG) *in vitro*. Field EPSPs (fEPSPs) evoked by stimulation of the perforant path (PP) were recorded extracellularly in the DG one week after a moderate impact applied by a fluid percussion injury (FPI) device. High frequency stimulation (HFS) of the PP caused LTP of the fEPSP-slope in slices from naïve and sham-operated rats, however, the LTP was strongly depressed in slices from FPI rats. Intraperitoneal administration of edaravone 15 min after FPI prevented the hyperactivities of DG neurons and attenuated impairment of the LTP in FPI rat dentate granular cells. In vitro application of spermine NONOate (sp-NO), a nitric oxide (NO) donor, for 30 min produced a gradual increase in the fEPSP-slope, lasting for more than 2 h. Edaravone attenuated the enhancement of the fEPSP-slope induced by sp-NO. After sp-NO treatment HFS could not produce an obvious LTP in the DG granule cell layer. Pretreatment of DG slices with edaravone prevented the sp-NO-induced impairment of LTP. These results suggest that administration of edaravone after FPI protects against post-traumatic impairment of LTP in granule cell layers of the DG, possibly by scavenging NO-related radicals.

Key words traumatic brain injury, long-term potentiation, hyperactivity, dentate granule cells, edaravone, neuroprotection, nitric oxide, free radical scavenger

INTRODUCTION

The neurological consequences of traumatic brain injury (TBI) are memory disturbance, cognitive impairment and chronic seizures that are related to the dysfunction of the hippocampal formation after head injury [1-3]. Fluid percussion injury (FPI) of the rat brain is the most extensively used and well characterized animal model of human TBI [4-6]. It has been shown that mossy neurons in the dentate gyrus (DG) were most vulnerable to various forms of injury, including epilepsy, ischemia and traumatic head injury [7-9]. Facilitation in the DG lowered thresholds for developing self-sustained seizure activity 1-12 weeks post-injury compared to sham-operated animals [9,10]. Functional studies showed that post-traumatic hyperactivity occurred in neurons of the hippocampal CA1 and the DG in FPI rats [7,11,12]. In the rat hippocampal CA1 area, impairment of long-term potentiation (LTP), which is thought to be a cellular model of memory function [13,14], has been shown in both *in vivo* [15,16] and *in vitro* prepara-

Correspondence to: Dr. Hiroshi Hasuo, Department of Physiology, Kurume University School of Medicine, 67 Asahi-machi, Kurume 830-0011, Japan. Tel: +81-942-31-7543 Fax: +81-942-31-7728 E-mail: hhasuo@med.kurume-u.ac.jp

Abbreviations: ACSF, artificial cerebrospinal fluid; CNS, central nervous system; DBCH, dormant basket cell hypothesis; DG, dentate gyrus; DL-APV, DL-2-Amino-5-phosphonovaleric Acid; fEPSP, field EPSP; FPI, fluid percussion injury; $GABA_A$ receptor, γ-aminobutyric acid receptor type A; HFS, high frequency stimulation; I-O curves, input-output relations; IPSP, inhibitory postsynaptic potential; Lt, left hemisphere; LTD, long-term depression; LTP, long-term potentiation; mPP, medial perforant path; NMDA, *n*-methyl-D-aspartate; NO, nitric oxide; ·OH, hydroxyl radical; PP, perforant path; pSpike, population spike; PSPs, postsynaptic potentials; RNS, reactive nitrogen species; ROS, reactive oxygen species; Rt, right hemisphere; sp-NO, spermine NONOate; TBI, traumatic brain injury.

tions [17-19]. Various molecular biological cascades have been reported to lead to cellular dysfunctions after TBI [20,21]. Nitric oxide (NO) not only mediates LTP and long-term depression (LTD) [22-24] but also causes direct neurotoxicity in central neurons [25,26]. Superoxide also has characteristic features, acting both as a functional messenger molecule for neuronal processes of LTP [27,28] and as a neurotoxic molecule [29-31]. Reactive free radicals, including reactive oxygen species (ROS) and reactive nitrogen species (RNS), are also implicated in the pathogenesis of various brain injuries, such as TBI, ischemia, and neurodegenerative disorders [31,32]. Edaravone (3-methyl-1-phenyl-2-pyrazolin-5-one: MCI-186) is a novel free radical scavenger clinically used as a neuroprotective agent against acute cerebral ischemia [33,34]. Edaravone is also shown to inhibit post-ischemic increases in hydroxyl radical (·OH) production and tissue injury in the penumbral or recirculated area in rat cerebral ischemia models [35,36]. Melatonin and phenylbutylnitrone, free radical scavengers, had protective effects against TBI via scavenging ROS and RNS [37-39]. We investigated the effect of edaravone on neuronal activity and LTP in the granule cell layer of the rat DG following head trauma. Preliminary findings of this work have appeared earlier [12].

MATERIALS AND METHODS

Surgical operation and FPI

Adult male Wistar rats were used for the entire study and were divided into 4 groups: one naïve group (n=20), one sham-operated group (n=18), one receiving lateral FPI (n=14), and one group receiving FPI with subsequent edaravone (n=12). This study was carried out in accordance with Kurume University's Guide for Animal Experimentation. FPI of the rat brain was carried out by the methods described previously [4,11,40]. Rats (230-260 g, n=26) were subjected to FPI at a moderate severity (4.2 atm) under pentobarbital anesthesia (50-60 mg/kg, i.p.). Edaravone (8 mg/kg) was administered trans-peritoneally 15 min after the FPI. The rat scalp was sagittally incised from bregma to lambda and a 3 mm hole was trephined in the skull at -3 mm (i.e. caudal) from the bregma, and 3.5 mm left of the sagittal suture. A leure-loc syringe hub with a 2.6 mm inside diameter was introduced through the hole, taking care not to compress the brain surface, and was bonded to the skull with cyanoacrylate adhesive. The hub was filled with saline before it was connected to the fluid percussion device. The fluid percussion device (HPD-1700: Dragonfly R & D, Inc., Ridgeley, WV, USA) consisted of a stainless steel cylinder with a 2.7 cm bore and a 7.6 cm piston stroke that was connected to the hub via high-pressure tubing. At the other end of the cylinder, a weighted pendulum arm was suspended a fixed distance above the head of the piston, which was sealed within the cylinder. Brain injury with moderate impact at a pressure of 4.2±0.1 atm was achieved by allowing the metal pendulum to strike the piston to inject a small volume of saline into the closed cranial cavity. The resulting pressure pulse was measured by a pressure transducer connected to a digital storage oscilloscope (DS-8608A, Iwatsu Test Instruments Co., Tokyo, Japan). The pH, pCO_2, PO_2 and O_2 saturation in arterial blood were measured 20-30 min after impact with an 850 pH/Blood Gas System (Bayer Medical Co., Ltd., Tokyo, Japan). The weights of rats before impact and 7 days later were not significantly different from those of naïve rats. No evidence of any behavioral seizure activity was seen 1-2 weeks after the FPI. Sham-operated rats were treated in the same way including connection to the FPI device, but the pendulum was not released.

Brain slice preparations

After a survival period of 1 week, the rats were deeply anaesthetized with pentobarbital sodium (50-65 mg/kg, i.p.) and killed by decapitation for slice experiments. Horizontal brain sections (400 μm in thickness) were cut from the ventral-to-mid section at −5.6 - −6.4 mm from bregma by a Vibroslice (Campden Instruments, Ltd., Loughborough, Leics., UK). The brain slices were left for 1 h to recover in oxygenated artificial cerebrospinal fluid (ACSF) at room temperature (22-24°C). The composition of the ACSF was as follows (in mM): NaCl, 117; KCl, 4.7; $CaCl_2$, 2.5; $MgCl_2$, 1.2; $NaHCO_3$, 25; $NaHPO_4$, 1.2 and D-glucose, 11 (299±4 mOsm).

Extracellular recording

Brain slices were continuously perfused with oxygenated ACSF at 30-32°C containing picrotoxin (100 μM), a $GABA_A$ receptor (γ-aminobutyric acid receptor type A) antagonist which blocks fast inhibitory postsynaptic potentials during recordings. Extracellular recordings were made from the DG granule cell layer with a glass microelectrode filled with 1 M NaCl (1-2 MΩ) (Fig. 1A). A bipolar-stimulating electrode was placed on the medial perforant path (mPP) in the molecular layers of the DG. The intensity of the test stimulus was chosen to yield a population spike (pSpike) of field EPSP (fEPSP) that was half the size necessary

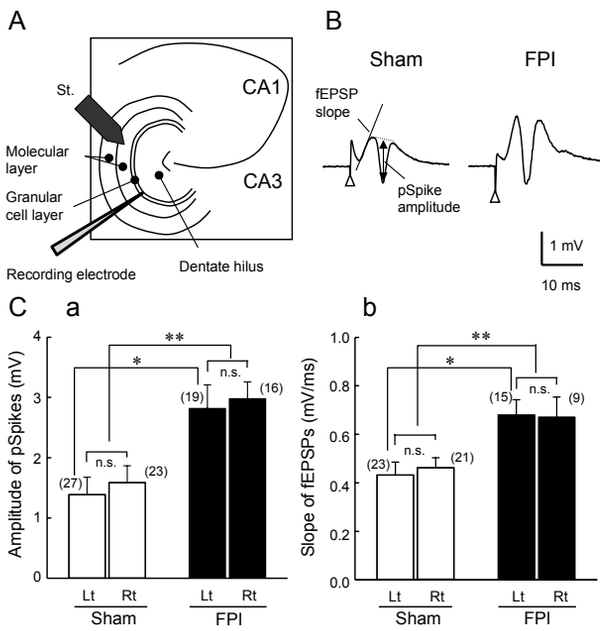

Fig. 1. Effects of FPI on the pSpike and fEPSP in the dentate granular cell layer. (A) Schematic diagram of horizontal section of the brain slice that includes the hippocampal formation and perforant path. Stimulus electrode was placed on the inner molecular layer of the DG (local stimulation) to stimulate the mPP. (B) Extracellular recordings of the field potentials in granule cell layer of the DG superfused with an ACSF containing picrotoxin (100 μM). Left and right traces were obtained by stimulus intensities of 10 V from sham-operated and FPI rats, respectively. A triangle indicates the time of stimulation. (C) Pooled data for the pSpike evoked by stimulus intensities of 10 V (a) and the fEPSP slope evoked by stimulus intensities of 6 V (b) obtained from sham-operated (open columns) and FPI (closed columns) rats, respectively. Data were obtained from the ipsilateral (Lt) and contralateral (Rt) hemispheres of the rat brain. Values are presented as mean±SEM. Vertical lines on each column represent SEM (*$p<0.05$, **$p<0.01$, n.s.; no significance). The number of slices is shown in parentheses.

to activate the maximum response (7-10 V for 200 μs). Six consecutive postsynaptic potentials (PSPs) were averaged. To induce LTP, high frequency stimulations (HFS; 100 Hz 0.1 s applied 6 trains every 10 s) were delivered at the necessary stimulus intensity to elicit a maximum response (usually 15-20 V for 200 μs). Evaluation of LTP was made at 30-50 min post-HFS and was expressed as the ratio of either the pSpike amplitude or the initial slope of fEPSP to the respective baseline responses obtained 20 min before the HFS. We used the pClamp system (Axon Instruments, Union city, CA, USA) operated by a computer (Dell, Round Rock, TX, USA) for data acquisition and later analysis.

Statistical analysis

Experimental data from different slices were pooled and presented as the mean±SEM (standard error of the mean). Differences between experimental and control values were tested using the unpaired Student's *t*-test; $p<0.05$ was accepted as statistically significant. Comparison of groups (more than three) were assessed by the one-way or two-way analysis of variance (ANOVA), followed by post-hoc test (the Dunn's method or the Holm-Sidak method) for multiple pairwise comparisons using SigmaPlot 11 software (Systat software, Inc., San Jose, CA, USA); $p<0.05$ was accepted as statistically significant.

RESULTS

Effects of FPI on neuronal excitability in the dentate granule cell layer

Extracellular field recordings in the dentate granule cell layer showed a somatic fEPSP associated with a pSpike following stimulation of the mPP (Fig. 1B). The minimal stimulus intensity needed to evoke visible fEPSPs (threshold) was obtained from the normal control (naïve) rats and sham-operated rats. The threshold for elicitation of the fEPSP was 2.0±0.1 V (n=16 slices) in 8 naïve rats and 2.1±0.1 V (n=18 slices) in 9 sham-operated rats. Similarly, the stimulation intensity that produced the minimum fEPSP was 2.1±0.2 V (n=32) in 14 FPI rats. These results suggest that there is no statistical difference in the threshold for fEPSP in naïve, sham-operated and FPI rats. In contrast, the amplitude of the pSpike in dentate granule cell layers in FPI rats was significantly enhanced compared with those in naïve and sham-operated rats (Fig. 1B). The pSpike amplitude evoked by a stimulus intensity of 10 V was 1.4±0.3 mV (n=27 slices) in sham-operated rats and 2.8±0.4 mV (n=19 slices) in FPI rats (Fig. 1C). The initial slope of the fEPSP evoked by a stimulus intensity of 6 V was 0.40±0.05 mV/ms (n=23) in sham-operated rats and 0.68±0.06 mV/ms (n=15) in slices from post-FPI rats. These differences were statistically significant ($p<0.05$). However, there was no significant difference in the amplitude of pSpike or the slope of the fEPSP between ipsilateral (left hemisphere; Lt) and contra-lateral (right hemisphere; Rt) dentate granule cell layers in either sham-operated or FPI rats. These data suggest that, under present experimental conditions, the effect

of the FPI on the excitatory synaptic transmission occurs bilaterally in the FPI rat DG. Therefore, comparisons between the values obtained from sham and FPI groups were made using pooled data from both Lt and Rt. The differences in both the amplitude of pSpike and the slope of fEPSP (Fig. 1C) were statistically significant ($p<0.01$).

Effect of FPI on LTP in the dentate granule cell layer

The time course and the magnitude of LTP in the dentate granule cell layer were determined in naïve, sham-operated and FPI rats. DG slices from each group were superfused with an ACSF containing picrotoxin (100 μM) to block $GABA_A$ receptors. When the HFS (6 trains of 10 pulses with frequency of 100 Hz every 10 s) was applied to the mPP, the pSpike amplitude of dentate granule cells gradually increased after tetanization over a period up to 8 min and then plateaued.

The enhancement of the amplitude lasted for more than 2 h, forming LTP in the sham-operated group (Fig. 2A). In these experiments, the average amplitudes of 60 consecutive pSpikes (10 min) were obtained before and 30 min after HFS. After delivery of the HFS to the mPP, the pSpike increased in amplitude to 270% of the control (before HFS) in sham-operated rats. The HFS-induced LTP in the DG was blocked by DL-2-Amino-5-phosphonovaleric Acid (DL-APV; 50 μM), a selective *n*-methyl-D-aspartate (NMDA) receptor antagonist (data not shown). Since previous studies have suggested that FPI erases the synaptic mechanisms required for LTP induction [15,16], LTP was compared between sham-operated and FPI rat groups. When HFS was applied to the mPP, a potentiation of the pSpike amplitude was seen in FPI rats. The average amplitude of 60 consecutive pSpikes obtained 30 min after HFS was approximately 150% of the control (before HFS). Figure 2B shows pooled data for LTP of the pSpike amplitude obtained 30 min after HFS in 9-14 slices. The magnitude of LTP was compared between naïve and sham-operated rats. HFS increased the amplitudes of pSpike to 272±26% (n=10 slices, Lt) and 254±16% (n=11 slices, Rt) of the control in the sham group, and 252±12% (n=9 slices, Lt) and 261±35% (n=10 slices, Rt) of the control in the naïve group (Fig. 2B). Thus, there was no significant difference in percent increase in the amplitude of pSpikes in the DG between sham-operated and naïve rats. These results suggest that sham-operation caused no significant depression of LTP in the dentate granule cell layer of the DG. In contrast, the amplitude of the pSpike was only 153±6% (n=14, Lt) and 151±13%

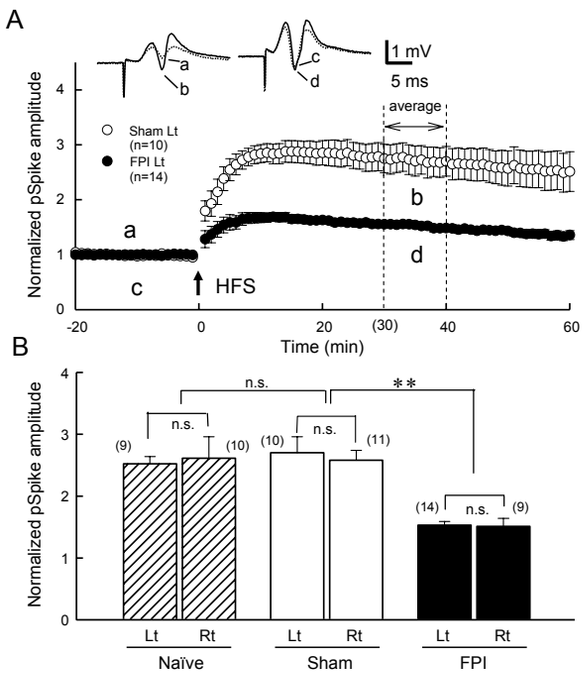

Fig. 2. Effects of FPI on the LTP in DG. (A) Time course of LTP of the pSpike amplitude in dentate granule cell layer obtained from sham-operated (open circles) and FPI (closed circles) rats. Upward arrow indicates the time for HFS of the mPP. Each symbol depicts the average amplitude of pSpike. Records (a-d) in insets were representative traces obtained at the time indicated by respective letters in the lower graph. All data were obtained from ipsilateral (Lt) hippocampal neurons. Vertical lines on each data point represent SEM. (B) Pooled data for LTP in ipsilateral (Lt) and contralateral (Rt) dentate granule cell layers in naïve (oblique columns), sham-operated (open columns) and FPI (closed columns) rats. The amplitude of pSpike was averaged between 30 and 40 min after the HFS. Values are presented as mean±SEM. Vertical lines on each column represent SEM (**$p<0.01$, n.s.; no significance). The number of slices is shown in parentheses.

(n=9, Rt) of the control in FPI rats. The percent increase in pSpike amplitude in FPI rats was smaller than that obtained from the sham-operated rat group (sham vs. FPI, $p<0.01$). Furthermore, LTP of the pSpike amplitude was similar in both Lt and Rt in FPI animals. These results suggest that fluid percussion causes functional disturbance of excitatory synapses that mediate the induction and maintenance of LTP in the dentate granule cell layer.

FPI produced a similar effect on LTP of the fEPSP slope in dentate granule cell layers. Figure 3A shows time courses of LTP determined by the fEPSP slopes in sham-operated and FPI rats. In this study, HFS

increased the slope of 60 consecutive fEPSPs to 150% (Lt) of control in sham-operated rats and 118% (Lt) of control in FPI rats (Fig. 3A). Pooled data from 10 slices in 5 rats showed that sham-operated rats responded to the HFS of the mPP with a long-lasting potentiation of the fEPSP slope by 141±7% (Lt) and 140±9% (Rt) of control (Fig. 3B). Percent increases in the fEPSP slope were 109±3% (Lt) of control and 104±7% (Rt) of control in 8-13 slices from 6 FPI rats. There was no difference between Lt and Rt in the DG.

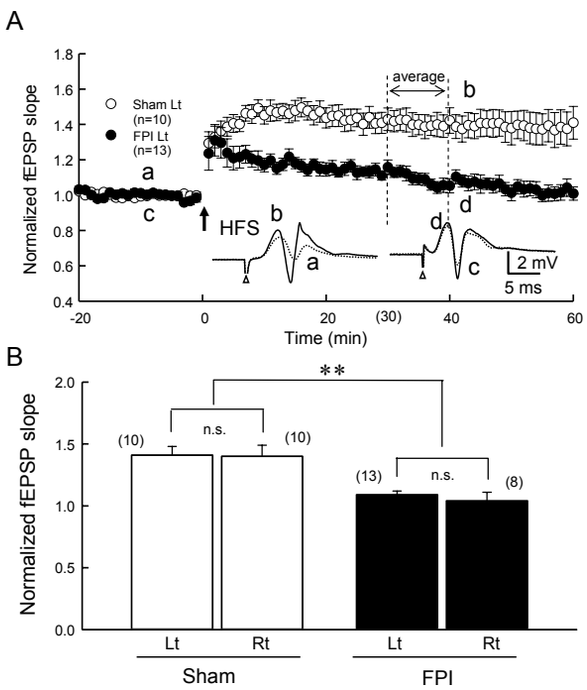

Fig. 3. LTP of fEPSP-slope taken in the dentate granular cell layer of sham-operated and FPI rats. DG slices were superfused with an ACSF containing picrotoxin (100 μM). (A) fEPSPs were evoked by single stimulation with an intensity of 6-9 V. Open and closed circles were obtained from sham-operated (n=10) and FPI (n=13) rats, respectively. The upward arrow indicated the time of HFS. Insets show sample records of the fEPSP obtained before and 40 min after HFS in sham (left traces) and FPI (right traces) groups, respectively. Records (a-d) were obtained at the times indicated by respective letters in the graph. (B) Pooled data for LTP of the fEPSP slope of ipsilateral (Lt) and contralateral (Rt) dentate granule cell layers in sham-operated and FPI rats. Each column indicates average value of normalized fEPSP slopes obtained between 30 and 40 min after HFS. Open and closed columns were obtained from sham-operated and FPI rats, respectively. Vertical lines on each column represent SEM (**$p<0.01$, n.s.; no significance). The number of slices is shown in parentheses.

Pooled data showed a significant difference between the values obtained from sham and FPI groups ($p<0.01$). These results suggest that at one week after FPI, the HFS could not generate LTP, as determined by the fEPSP slope in dentate granule cell layers.

Effect of edaravone on neuronal activity in dentate granule cells

The post-traumatic hyperexcitability of synaptic transmission was examined in FPI rats with i.p. administration of edaravone (8 mg/kg), a free radical scavenger, 15 min after FPI. The rectal temperature of FPI rats was not significantly altered (37.4±0.2°C, n=7) after the administrations of edaravone. As a control study, we examined the effect of i.p. administration of edaravone on the neuronal activity in sham-operated rats. The pSpike amplitude in sham-operated rats showed no obvious changes 1 week after the administration of edaravone (8 mg/kg, i.p.) or saline (as vehicle) in dentate granule cells (data not shown). Figure 4A shows sample records of the field potentials elicited by stimuli of mPP with intensities between 1 to 10 V in sham-operated rats, FPI rats, and those with i.p. administration of edaravone. The fEPSP slopes (mV/ms) were plotted against the intensity of stimuli (Vi) in sham-operated, FPI alone, and FPI rats treated with edaravone (Fig. 4B). The slope of the input-output relation (I-O curve) was evaluated individually by a linear regression program using the values obtained by the stimuli between 3 and 6 Vi, since the I-O curves showed high linearities at these range of stimuli. These I-O curves in ipsi- and contra-lateral dentate granular cell layers of sham-operated groups had slopes of 0.08±0.01 mV/ms vs. Vi (n=23, Lt) and 0.10±0.01 mV/ms vs. Vi (n=21, Rt), respectively. In contrast, the slopes of the I-O curve for the FPI alone groups were increased to 0.19±0.02 mV/ms vs. Vi (n=11, Lt) and 0.17±0.02 mV/ms vs. Vi (n=9, Rt). In FPI rats after i.p. administration of edaravone, however, the slopes of the I-O curve of the fEPSP recovered to 0.10±0.01 mV/ms vs. Vi (n=13, Lt) and 0.08±0.01 mV/ms vs. Vi (n=8, Rt). Comparisons of the I-O curves were made using the 1-10 Vi data by two-way ANOVA. The values of the I-O curve for the FPI groups were significantly greater than those for the sham-operated group ($p<0.01$), indicating that FPI causes post-traumatic hyperexcitability of dentate granule cells. There was no statistical difference in the I-O curves between Rt and Lt. The I-O curves in FPI rats treated with edaravone were almost identical to those of sham-operated rats (Fig. 4B). Thus, i.p. administration of edaravone prevented the development of post-traumatic hyperexcitability of DG neurons.

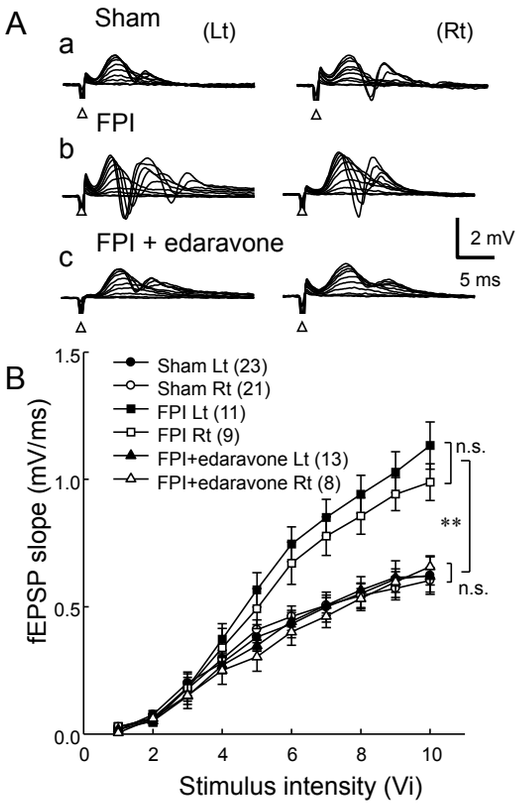

Fig. 4. Effects of edaravone on the hyperexcitability of dentate neurons after FPI. (A) The representative traces of field potentials which were obtained from sham-operated (a), FPI alone (b) and FPI with edaravone (c) rats. Intensity of stimuli was increased from 1 V to 10 V in 1 V increments. Left and right traces were obtained from Lt and Rt, respectively. (B) Graph shows the relationship between the initial slope of fEPSPs (mV/ms) and the intensity of stimulations (Vi) in the granule cell layer in the DG. The fEPSP was evoked by stimulation of the mPP with intensities of 1-10 V. Circles, squares and triangles were obtained from sham-operated, FPI and FPI rats with i.p. administration of edaravone, respectively. Closed and open symbols were taken from Lt and Rt, respectively. Values are presented as mean±SEM. Vertical lines on each data point represent SEM (**$p<0.01$, n.s.; no significance, two-way ANOVA). The number of slices is shown in parentheses.

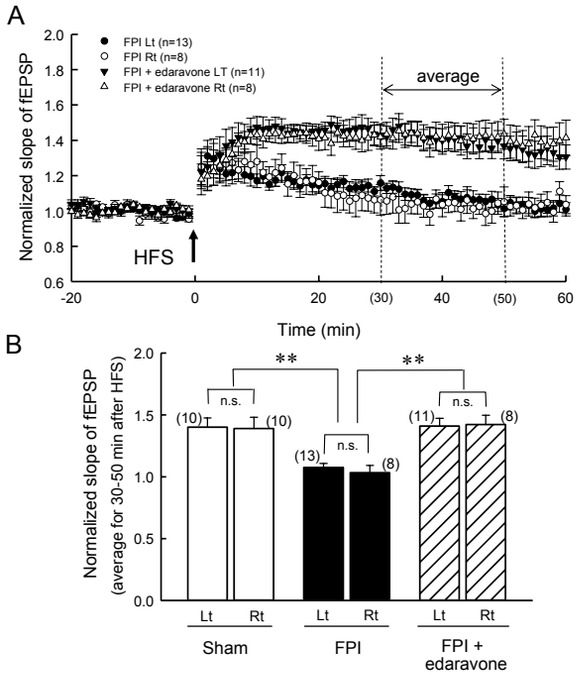

Fig. 5. Effects of i.p. administration of edaravone on the LTP of fEPSP in DG neurons. (A) Time course of the LTPs obtained from FPI alone (circles) and FPI rats with application of edaravone (triangles). Closed and open symbols were obtained from Lt and Rt hemisphere of rat brain, respectively. The number of slices is shown in parentheses. (B) Pooled data for the effect of i.p. administration of edaravone on the LTP. Open and closed and oblique columns were taken from sham-operated, FPI alone and FPI with edaravone groups, respectively. Right and left columns of each pair were obtained from right (Rt) and left (Lt) hemisphere of rat brain, respectively. Vertical lines on each column represent SEM (**$p<0.01$, n.s.; no significance).

Effects of edaravone on LTP in dentate granule cell layers

LTP profiles were compared in FPI rats and those with i.p. administration of edaravone. In these experiments, brain slices were treated with picrotoxin (100 μM) to block $GABA_A$ receptors. Figure 5A shows the time courses of LTP of the fEPSP slope in FPI rats and FPI rats with edaravone treatment. In the FPI alone group, the slope of fEPSPs returned to the baseline control level within 60 min after the HFS. However, the slope of fEPSP was still enhanced at 60 min after the HFS in FPI rats after i.p. administration of edaravone. Figure 5B shows pooled data for the effect of edaravone on the LTP determined by fEPSP slope, obtained 30-50 min after the HFS, in ipsi- and contralateral dentate granule cell layers. The magnitude of LTP was 140±7% (n=10, Lt) of control in sham-operated, 108±3% (n=13, Lt) of control in FPI only, and 141±6% (n=11, Lt) of control in FPI followed by edaravone treatment. The fEPSP slopes in contra-lateral dentate granular neurons were 139±9% (n=10, Rt) in sham-operated rats, 103±6% (n=8, Rt) in FPI rats and 142±8% (n=8, Rt) in FPI rats with edaravone

(Fig. 5B). Pooled data showed a significant difference between the values obtained from the FPI-alone group and the FPI-treated with edaravone group. The edaravone treated group showed an LTP profile that was almost identical to that of the sham-operated group. These results suggest that i.p. administration of edaravone 15 min after FPI improves the post-traumatic impairment of LTP in the granule cell layer of the DG.

Effects of bath-application of spermine NONOate (sp-NO) and edaravone on the fEPSPs in the dentate granular cell layers

It has been shown that NO not only promotes or mediates LTP and/or LTD [22] but also causes direct neurotoxicity in central neurons [25,26]. It is important to know whether NO is related to the post-traumatic neuronal hyperexcitability and impairment of LTP in DG neurons. In addition, it has been reported that edaravone scavenges NO [41]. We examined the acute effects of NO donor and free radical scavenger on the fEPSP slope in dentate granule cells of naïve rats. Figure 6A shows the effect of bath-application of sp-NO, a NO donor, on the fEPSP slope in the dentate granular cell layer of naïve rats. Bath-application of sp-NO (100 μM) for 30 min increased the initial slope of the fEPSP in the absence of edaravone (100 μM) (Fig. 6A, open circles). In these experiments, the I-O curves of fEPSP were examined. Figure 6B shows the data obtained before and 50 min after application of sp-NO. After treatment of sp-NO, the normalized slope of fEPSP at 10 V stimulus increased to 1.51±0.20 (n=8). The I-O curve obtained after sp-NO treatment was significantly different from the control ($p<0.05$). The enhancement of the fEPSP slope developed within 60 min and was maintained for more than 120 min even after removal of sp-NO from the external solution. Pooled data showed that sp-NO (100 μM) enhanced the fEPSP slope to 135±9% (n=9 slices) of control (Fig. 6C, open column). These results suggest that sp-NO produces a long-lasting enhancement of the fEPSP slope in the dentate granule cell layer. The effect of sp-NO (100 μM) on the fEPSP slope was also examined in the presence of edaravone (100 μM) in the dentate granule cell layer (Fig. 6A). Brain slices were first superfused with an external solution containing edaravone (100 μM) for 20 min, and then sp-NO (100 μM) was added to the edaravone (100 μM)-containing ACSF for 30 min. Bath-application of edaravone itself produced no obvious change in the slope of fEPSP. Application of sp-NO (100 μM) for 30 min did not consistently produce enhancement of the fEPSP slope in the presence of edaravone (100 μM) (Fig. 6A, closed circles). Pooled data showed that the fEPSP slope was 102±3% (n=5) of control in DG slices treated with both edaravone (100 μM) and sp-NO (100 μM) (Fig. 6C, closed column). This value

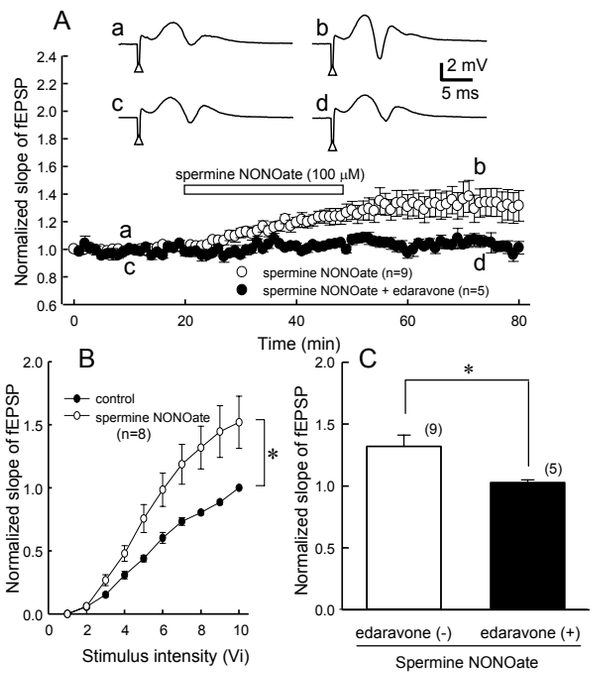

Fig. 6. Effect of *in vitro* administration of sp-NO and edaravone on the slope of fEPSPs. Experiments were done using DG slices of naïve rats. (A) Time course of the facilitation in the slope of fEPSP induced by bath-application of sp-NO (100 μM). Circles indicate the average value of normalized slope of fEPSPs. Open and closed circles were obtained in the absence or in the presence of edaravone (100 μM), respectively. Open horizontal bar indicates the period of the application of sp-NO (100 μM) to the ACSF. The slope of fEPSP obtained before application of sp-NO was indicated as 1. Sp-NO (100 μM) was added to an ACSF containing edaravone (100 μM). Records (a-d) in insets were representative traces obtained at the time indicated by respective letters in lower graph. (B) Pooled data for the input-output relations of the normalized slope of fEPSP before (closed circles) and after treatment of sp-NO (open circles). The slope of fEPSP at 10 V stimulus was indicated as 1. Vertical lines on each symbol represent SEM (*$p<0.05$, two-way ANOVA) (C) Pooled data for the effect of sp-NO (100 μM) on the slope of fEPSP. Open and closed columns were taken in the absence and the presence of edaravone (100 μM), respectively. The slope of fEPSP obtained before application of drugs was indicated as 1. Vertical lines on each column represent SEM (*$p<0.05$). The number of slices is shown in parentheses.

was significantly different from that obtained in the absence of edaravone (Fig. 6C, $p<0.05$). These results suggest that edaravone attenuates the NO-induced enhancement of fEPSP slope in the dentate granular cell layer.

Effects of in vitro administration of edaravone and sp-NO on LTP in dentate granule cell layers

Brain slices were superfused with an ACSF containing picrotoxin (100 μM) to block fast IPSPs. Application of HFS to the mPP produced a long-lasting enhancement of the fEPSP slope for more than 2 h, producing typical LTP in naïve rats (data not shown). Pooled data showed that the magnitude of LTP in the fEPSP slope was 141±6% (n=11 slices) of control in 6 naïve rats (Fig. 7B). Figure 7A shows the effects of pre-treatment of sp-NO (100 μM) alone (open circles) and sp-NO (100 μM) with edaravone (100 μM) (closed circles) for 30 min on LTP in dentate granular cell layers. After treatment with sp-NO (100 μM) alone, the HFS produced a transient decrease in the fEPSP slope (70% of control, n=9) that recovered within 10 min and then repotentiated (122% of control, n=9). However, the slope of fEPSP returned to the baseline level (before HFS level) within 60 min. Pooled data showed that the slope of the fEPSP obtained 40-50 min after HFS was 106±3% (n=9) of the control in the presence of sp-NO (100 μM) (Fig. 7B, oblique column). These results suggest that NO production by sp-NO (100 μM) suppresses induction of LTP in dentate granule cell layers. The effect of sp-NO (100 μM) on LTP was also examined in the presence of edaravone (100 μM) in dentate granule cell layers. Application of edaravone (100 μM) to the external solution for 30 min produced no effect on the fEPSP slope in granule cell layers. Sp-NO (100 μM) was then added to edaravone-containing external solution. In the presence of both edaravone (100 μM) and sp-NO (100 μM), HFS of the perforant path enhanced the fEPSP slope to 150% of the control 40-50 min after HFS, producing LTP (Fig. 7A closed circles). Figure 7B (closed column) shows pooled data for the effect of *in vitro* application of both edaravone (100 μM) and sp-NO (100 μM) on LTP of fEPSP slope. Under these experimental conditions, the magnitude of LTP of fEPSP slope was 154±12% (n=5 slices), which was significantly different from the value after sp-NO treatment alone. The effect of bath-application of edaravone alone on the HFS-induced LTP was investigated. The magnitudes of the LTP in the presence of edaravone (100 μM or 500 μM) were 133±10% (n=7) for 100 μM and 112±5 % (n=4) for 500 μM, respectively (data not shown). The value for edaravone (500 μM) was significantly different from the control value. These results suggest that edaravone attenuates the sp-NO-induced depression of LTP, probably by blocking NO-dependent processes of induction and maintenance of LTP in the granule cell layer of the DG. These results indicate that i.p. administration of edaravone at an early period after FPI may be effective in preventing post-traumatic impairment of LTP.

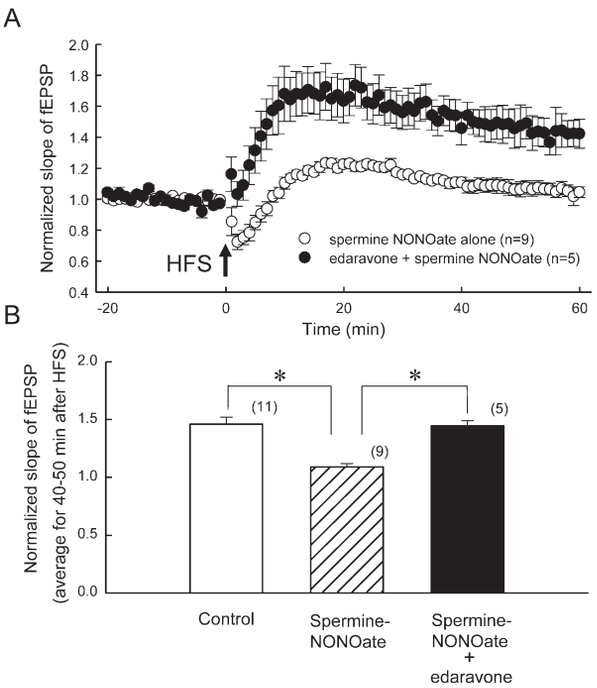

Fig. 7. Effect of *in vitro* administration of sp-NO on the LTP of fEPSP in granular neurons of DG. (A) Time course of the fEPSP slope obtained before and after application of the HFS to the perforant path. Experiments were done using DG slices of naïve rats. Open and closed circles indicate the data obtained in the presence of sp-NO (100 μM) alone and in the presence of both edaravone (100 μM) and sp-NO (100 μM), respectively. The time of the HFS is indicated by an upward arrow. The mean slope of fEPSP obtained before application of HFS was indicated as 1. Values are presented as mean± SEM. (B) Pooled data for the magnitudes of LTP obtained from control slices, sp-NO (100 μM) alone treated slices, and both edaravone (100 μM) and sp-NO (100 μM) treated slices, respectively. Vertical lines on column represent SEM (*$p<0.05$). The number of slices is shown in parentheses.

DISCUSSION

The present study showed that 1) FPI enhanced

the fEPSP slope and the pSpike amplitude, 2) FPI suppressed the induction and maintenance of LTP in the fEPSP and the pSpike, and 3) i.p. administration of edaravone in the early post-traumatic period (15 min after the FPI) prevented the hyperactivity of neurons and the impairment of LTP in bilateral dentate granule cell layers. The enhancement of the fEPSP slope and the pSpike amplitude following FPI was associated with no obvious change in the threshold for their generation in the granule cell layer of the DG. The slope of the I-O curve was increased in FPI rats as compared with sham-operated rats. These results suggest that the efficacy of excitatory synaptic transmission is enhanced in the dentate granule cell layer after FPI. FPI has been shown to enhance the excitatory synaptic function in hippocampal CA1 neurons of FPI rats [11,40]. As regards the mechanism of post-traumatic hyperexcitability, several hypotheses have appeared in regard to the DG. Santhakumar et al. [42] have reported an 'irritable mossy cells hypothesis' in DG neurons. Increased discharge of granule cells driven by a hyperexcitable feedback pathway from mossy hilar cells results in the development of post-traumatic seizures and memory deficits. Surviving mossy hilar cells mainly contribute to the hyperexcitability of dentate granule cells after the FPI. Sloviter [43,44] proposed a 'dormant basket cell hypothesis (DBCH)' that described the importance of mossy cell degeneration in the DG. Persistent increase in glutamate release from the perforant path leads to a decrease in the excitation of inhibitory interneurons, resulting in the disinhibition of excitatory granule cells. In connection to the hyperexcitability of mossy hilar cells after head trauma, mossy fiber synaptic reorganization has been demonstrated in human temporal-lobe epilepsy [45]. This plasticity includes an early and persistent abnormal sprouting of granule cell axons (mossy fibers) synapsing in the molecular layer [46,47]. Our previous study has suggested that the post-traumatic hyperexcitability in the hippocampal CAl neurons is caused at least in part by the facilitation of glutamatergic transmission [11]. The results in the present study also suggest that FPI causes hyperactivity of excitatory synaptic transmission in rat dentate granular cell layers lasting at least 1 week after FPI.

LTP, a long-lasting synaptic plasticity, is the experimental paradigm of the cellular basis for learning and memory [13,14,48]. A previous study showed that the enhancement of inhibitory synaptic activity reduced hyperexcitability in hippocampal CA1 neurons in FPI rats [40]. The depression of LTP in dentate granule cell layers was not related to the disinhibition after FPI, because DG slices were superfused with an ACSF containing picrotoxin, an inhibitor for $GABA_A$ receptors. One of the most interesting findings of the present study was the co-existence of the impairment of LTP and the enhancement of the fEPSP in the dentate granule cell layer following FPI. It has been proposed that one of the likely mechanisms for the lack of induction of LTP is probably LTP itself, because pathways previously enhanced by FPI, a pathological form of LTP, cannot endure successive LTP [18,49]. It has been known that the NMDA receptor-dependent pathway is closely related to injury-induced LTP impairment in mouse hippocampal CA1 after TBI [21]. The initial response to brain injury is an indiscriminant recurrent release of excitatory neurotransmitters, leading to widespread depolarization [50-52] that consequently releases the voltage-sensitive magnesium block of the NMDA receptors [53]. Moreover, Zhang et al. [54] have demonstrated relief from magnesium block of the NMDA receptors following mechanical injury to cortical neurons. The large and sudden increase in extracellular glutamate after a brain injury would result in an increase in Ca^{2+} influx to the intracellular space, leading to pathologic LTP. The hyperactivity of excitatory synaptic transmission may occlude subsequent LTP induction in dentate granule cell layers.

Various molecular biological cascades have been reported to be involved in the process of the induction and maintenance of LTP after TBI [20,21]. NO not only acts as a direct neurotoxic molecule [25,26], but also promotes or mediates LTP or LTD [22-24]. ROS, including superoxide, also exhibit two opposite features, such as neurotoxity [31], while also functioning as messenger molecules in neuronal processes of synaptic plasticity [28,55]. LTP of synaptic transmission in area CA1 of the hippocampus is dependent on superoxide and is occluded by the superoxide-induced potentiation of synaptic transmission [28,56]. NO is known to react with ROS to generate RNS that also cause neuronal cell death through oxidation [32]. Brain injury generates ROS at the early post-traumatic period that spread through the vulnerable central nervous system (CNS) producing the deleterious consequences of brain injuries [31]. It has been shown that melatonin and phenylbutylnitrone, free radical scavengers, had protective effects against TBI via scavenging of ROS and RNS [37-39]. Edaravone is also a free radical scavenger clinically used as a neuroprotective agent against acute cerebral ischemia [33,34]. Edaravone inhibits post-ischemic increases in ·OH production and tissue injury in the penumbral or recirculated area in rat cerebral ischemia models [35,36].

In addition, it has been reported that edaravone scavenges NO [41]. The present study showed that i.p. administration of edaravone attenuated the FPI-induced enhancement of the fEPSP and the impairment of LTP in dentate granule cell layers. The lack of induction of LTP after brain injury may be due to post-traumatic increase in NO and/or free radicals, because previous enhancement of these molecules by FPI may suppress any further LTP. Such a pathological enhancement of the function of excitatory synapses would prevent subsequent LTP induction in dentate granule cells. We, therefore, hypothesized that edaravone prevented the pathological form of LTP following brain injury in dentate granule cell layers by suppressing the NO-ROS pathway. The present study examined the effect of sp-NO, a NO donor, on the induction of LTP in brain slice preparations, *in vitro*. Bath-application of sp-NO (100 μM) produced a long-lasting increase in the fEPSP slope in dentate granule cell layers. Such an enhancement of fEPSP slope was blocked by pretreatment with edaravone (100 μM). The present study also showed that HFS produced no additional enhancement of the fEPSP in dentate granule cells in the slices pretreated with sp-NO (100 μM) alone for 30 min. These results may be due to NO and/or NO-stimulated free radical production, because application of edaravone attenuated sp-NO-induced enhancement of the fEPSP slope and prevented the impairment of LTP of the fEPSP slope in FPI rats. Although the precise mechanisms of edaravone on the FPI-induced impairment of LTP were not fully elucidated, i.p. administration of edaravone in the early post-traumatic period prevented the impairment of LTP in the rat DG. The results of the present study suggest a therapeutic potential of edaravone against post-traumatic impairment of cognitive functions at brain injury by scavenging NO and/or free radicals.

ACKNOWLEDGMENTS: The authors are grateful to Mr. G. Wyckoff for reading the manuscript and his useful comments during the present study. This work was partially supported by JSPS KAKENHI, Grant-in-Aid for Scientific Research (C) (17500279 and 20591698). This research was also supported from the Ministry of Education, Culture, Sports, Science and Technology as a part of a project for establishing open research centers in private universities.

REFERENCES

1. Capruso DX, and Levin HS. Cognitive impairment following closed head injury. Neurol Clin 1992; 10:879-893.
2. Rempel-Clower NL, Zola SM, Squire LR, and Amaral DG. Three cases of enduring memory impairment after bilateral damage limited to the hippocampal formation. J Neurosci 1996; 16:5233-5255.
3. Annegers JF, Hauser WA, Coan SP, and Rocca WA. A population-based study of seizures after traumatic brain injuries. N Engl J Med 1998; 338:20-24.
4. Dixon CE, Lyeth BG, Povlishock JT, Findling RL, Hamm RJ et al. A fluid percussion model of experimental brain injury in the rat. J Neurosurg 1987; 67:110-119.
5. McIntosh TK, Vink R, Noble L, Yamakami I, Fernyak S et al. Traumatic brain injury in the rat: characterization of a lateral fluid-percussion model. Neuroscience 1989; 28:233-244.
6. Thompson HJ, Lifshitz J, Marklund N, Grady MS, Graham DI et al. Lateral fluid percussion brain injury: a 15-year review and evaluation. J Neurotrauma 2005; 22:42-75.
7. Lowenstein DH, Thomas MJ, Smith DH, and McIntosh TK. Selective vulnerability of dentate hilar neurons following traumatic brain injury: a potential mechanistic link between head trauma and disorders of the hippocampus. J Neurosci 1992; 12:4846-4853.
8. Toth Z, Hollrigel GS, Gorcs T, and Soltesz I. Instantaneous perturbation of dentate interneuronal networks by a pressure wave-transient delivered to the neocortex. J Neurosci 1997; 17:8106-8117.
9. Coulter DA, Rafiq A, Shumate M, Gong QZ, DeLorenzo RJ et al. Brain injury-induced enhanced limbic epileptogenesis: anatomical and physiological parallels to an animal model of temporal lobe epilepsy. Epilepsy Res 1996; 26:81-91.
10. Santhakumar V, Ratzliff ADH, Jeng J, Toth Z, and Soltesz I. Long-term hyperexcitability in the hippocampus after experimental head trauma. Ann Neurol 2001; 50:708-717.
11. Cao R, Hasuo H, Ooba S, Akasu T, and Zhang X. Facilitation of glutamatergic synaptic transmission in hippocampal CA1 area of rats with traumatic brain injury. Neurosci Lett 2006; 401:136-141.
12. Yamashita S, Ooba S, Orito K, Hasuo H, Tokutomi T et al. Edaravone effectively improve the neuronal dysfunction induced by lateral fluid percussion injury in rats. Neurotrauma Res 2006; 18:35-40.
13. Bliss TVP, and Collingridge GL. A synaptic model of memory: long-term potentiation in the hippocampus. Nature 1993; 361:31-39.
14. Lynch MA. Long-term potentiation and memory. Physiol Rev 2004; 84:87-136.
15. Miyazaki S, Katayama Y, Lyeth BG, Jenkins LW, DeWitt DS et al. Enduring suppression of hippocampal long-term potentiation following traumatic brain injury in rat. Brain Res 1992; 585:335-339.
16. Reeves TM, Lyeth BG, and Povlishock JT. Long-term potentiation deficits and excitability changes following traumatic brain injury. Exp Brain Res 1995; 106:248-256.
17. Sick TJ, Pérez-Pinzón MA, and Feng ZZ. Impaired expression of long-term potentiation in hippocampal slices 4 and 48 h following mild fluid-percussion brain injury in vivo. Brain Res 1998; 785:287-292.
18. D'Ambrosio R, Maris DO, Grady MS, Winn HR, and Janigro D. Selective loss of hippocampal long-term potentiation, but not depression, following fluid percussion injury. Brain Res 1998; 786:64-79.
19. Sanders MJ, Sick TJ, Perez-Pinzon MA, Dietrich WD, and

Green EJ. Chronic failure in the maintenance of long-term potentiation following fluid percussion injury in the rat. Brain Res 2000; 861:69-76.
20. Atkins CM, Chen S, Alonso OF, Dietrich WD, and Hu BR. Activation of calcium/calmodulin-dependent protein kinases after traumatic brain injury. J Cereb Blood Flow Metab 2006; 26:1507-1518.
21. Schwarzbach E, Bonislawski DP, Xiong G, and Cohen AS. Mechanisms underlying the inability to induce area CA1 LTP in the mouse after traumatic brain injury. Hippocampus 2006; 16:541-550.
22. Schuman EM, and Madison DV. A requirement for the intercellular messenger nitric oxide in long-term potentiation. Science 1991; 254:1503-1506.
23. Meffert MK, Haley JE, Schuman EM, Schulman H, and Madison DV. Inhibition of hippocampal heme oxygenase, nitric oxide synthase, and long-term potentiation by metalloporphyrins. Neuron 1994; 13:1225-1233.
24. Gage AT, Reyes M, and Stanton PK. Nitric-oxide-guanylyl-cyclase-dependent and -independent components of multiple forms of long-term synaptic depression. Hippocampus 1997; 7:286-295.
25. Dawson VL, Kizushi VM, Huang PL, Snyder SH, and Dawson TM. Resistance to neurotoxicity in cortical cultures from neuronal nitric oxide synthase-deficient mice. J Neurosci 1996; 16:2479-2487.
26. Barth A, Newell DW, Nguyen LB, Winn HR, Wender R et al. Neurotoxicity in organotypic hippocampal slices mediated by adenosine analogues and nitric oxide. Brain Res 1997; 762:79-88.
27. Klann E. Cell-permeable scavengers of superoxide prevent long-term potentiation in hippocampal area CA1. J Neurophysiol 1998; 80:452-457.
28. Knapp LT, and Klann E. Potentiation of hippocampal synaptic transmission by superoxide requires the oxidative activation of protein kinase C. J Neurosci 2002; 22:674-683.
29. Demopoulos HB, Flamm ES, Pietronigro DD, and Seligman ML. The free radical pathology and the microcirculation in the major central nervous system disorders. Acta Physiol Scand Suppl 1980; 492:91-119.
30. Siesjö BK. Cell damage in the brain: a speculative synthesis. J Cereb Blood Flow Metab 1981; 1:155-185.
31. Lewén A, Matz P, and Chan PH. Free radical pathways in CNS injury. J Neurotrauma 2000; 17:871-890.
32. Pannu R, and Singh I. Pharmacological strategies for the regulation of inducible nitric oxide synthase: neurodegenerative versus neuroprotective mechanisms. Neurochem Int 2006; 49:170-182.
33. Otani H, Togashi H, Jesmin S, Sakuma I, Yamaguchi T et al. Temporal effects of edaravone, a free radical scavenger, on transient ischemia-induced neuronal dysfunction in the rat hippocampus. Eur J Pharmacol 2005; 512:129-137.
34. Yoshida H, Yanai H, Namiki Y, Fukatsu-Sasaki K, Furutani N et al. Neuroprotective effects of edaravone: a novel free radical scavenger in cerebrovascular injury. CNS Drug Rev 2006; 12:9-20.
35. Watanabe T, Yuki S, Egawa M, and Nishi H. Protective effects of MCI-186 on cerebral ischemia: possible involvement of free radical scavenging and antioxidant actions. J Pharmacol Exp Ther 1994; 268:1597-1604.
36. Yamamoto T, Yuki S, Watanabe T, Mitsuka M, Saito KI et al. Delayed neuronal death prevented by inhibition of increased hydroxyl radical formation in a transient cerebral ischemia. Brain Res 1997; 762:240-242.
37. Marklund N, Clausen F, McIntosh TK, and Hillered L. Free radical scavenger posttreatment improves functional and morphological outcome after fluid percussion injury in the rat. J Neurotrauma 2001; 18:821-832.
38. Samuelsson C, Kumlien E, Elfving Å, Lindholm D, and Ronne-Engström E. The effects of PBN (phenyl-butyl-nitrone) on GLT-1 levels and on the extracellular levels of amino acids and energy metabolites in a model of iron-induced posttraumatic epilepsy. Epilepsy Res 2003; 56:165-173.
39. Ozdemir D, Tugyan K, Uysal N, Sonmez U, Sonmez A et al. Protective effect of melatonin against head trauma-induced hippocampal damage and spatial memory deficits in immature rats. Neurosci Lett 2005; 385:234-239.
40. Ooba S, Hasuo H, Shigemori M, and Akasu T. Diazepam attenuates the post-traumatic hyperactivity of excitatory synapses in rat hippocampal CA1 neurons. Neurosci Res 2008; 62:195-205.
41. Satoh K, Ikeda Y, Shioda, S, Tobe T, and Yoshikawa T. Edaravone scavenges nitric oxide. Redox Rep 2002; 7:219-222.
42. Santhakumar V, Bender R, Frotscher M, Ross ST, Hollrigel GS et al. Granule cell hyperexcitability in the early post-traumatic rat dentate gyrus: the 'irritable mossy cell' hypothesis. J Physiol 2000; 524:117-134.
43. Sloviter RS. Permanently altered hippocampal structure, excitability, and inhibition after experimental status epilepticus in the rat: the "dormant basket cell" hypothesis and its possible relevance to temporal lobe epilepsy. Hippocampus 1991; 1:41-66.
44. Sloviter RS. On the relationship between neuropathology and pathophysiology in the epileptic hippocampus of humans and experimental animals. Hippocampus 1994; 4:250-253.
45. Babb TL. Axonal growth and neosynaptogenesis in human and experimental hippocampal epilepsy. Adv Neurol 1997; 72:45-51.
46. Frotscher M, and Zimmer J. Lesion-induced mossy fibers to the molecular layer of the rat fascia dentata: identification of postsynaptic granule cells by the Golgi-EM technique. J Comp Neurol 1983; 215:299-311.
47. Sutula T, He XX, Cavazos J, and Scott G. Synaptic reorganization in the hippocampus induced by abnormal functional activity. Science 1988; 239:1147-1150.
48. Bliss TVP, and Lømo T. Long-lasting potentiation of synaptic transmission in the dentate area of the anaesthetized rabbit following stimulation of the perforant path. J Physiol 1973; 232:331-356.
49. Obrenovitch TP, and Urenjak J. Altered glutamatergic transmission in neurological disorders: from high extracellular glutamate to excessive synaptic efficacy. Prog Neurobiol 1997; 51:39-87.
50. Faden AI, Demediuk P, Panter SS, and Vink R. The role of excitatory amino acids and NMDA receptors in traumatic brain injury. Science 1989; 244:798-800.
51. Katayama Y, Becker DP, Tamura T, and Hovda DA. Massive increases in extracellular potassium and the indiscriminate

release of glutamate following concussive brain injury. J Neurosurg 1990; 73:889-900.
52. Hayes RL, Jenkins LW, and Lyeth BG. Neurotransmitter-mediated mechanisms of traumatic brain injury: acetylcholine and excitatory amino acids. J Neurotrauma 1992; 9:S173-S187.
53. Nowak L, Bregestovski P, Ascher P, Herbet A, and Prochiantz A. Magnesium gates glutamate-activated channels in mouse central neurones. Nature 1984; 307:462-465.
54. Zhang L, Rzigalinski BA, Ellis EF, and Satin LS. Reduction of voltage-dependent Mg^{2+} blockade of NMDA current in mechanically injured neurons. Science 1996; 274:1921-1923.
55. Thiels E, Urban NN, Gonzalez-Burgos GR, Kanterewicz BI, Barrionuevo G et al. Impairment of long-term potentiation and associative memory in mice that overexpress extracellular superoxide dismutase. J Neurosci 2000; 20:7631-7639.
56. Klann E, Roberson ED, Knapp LT, and Sweatt JD. A role for superoxide in protein kinase C activation and induction of long-term potentiation. J Biol Chem 1998; 273:4516-4522.

Case Report

Kurume Medical Journal, 58, 59-61, 2011

Can Renal Infarction Occur After Renal Cyst Aspiration? Case Report

HABIB EMRE, YASEMIN USUL SOYORAL, SERHAT TANIK*, ILHAN GECIT*, HUSEYIN BEGENIK, NECIP PIRINCCI* AND REHA ERKOC

Department of Nephrology and Urology, Yuzuncu Yil University,Van 65100, Turkey*

Received 26 March 2011, accepted 10 May 2011

Summary: Renal infarction (RI) is a rarely seen disorder, and the diagnosis is often missed. The two major causes of RI are thromboemboli originhating from a thrombus in the heart or aorta, and in-situ thrombosis of a renal artery. We report a case of RI that developed due to renal artery and vein thrombosis, as confirmed by pathological evaluation of the nephrectomy material, three weeks after renal cyst aspiration.

Key words renal infarction, cyst aspiration, acute renal failure, lactate dehydrogenase, nephrectomy

INTRODUCTION

The detection of renal infarction (RI) can be delayed or missed because the condition is rare, and its clinical presentation is nonspecific and similar to other more common disorders such as pyelonephritis or urolithiasis. The two major causes of RI are thromboemboli originating from a thrombus in the heart or aorta, and in-situ thrombosis of a renal artery, which is less common [1,2]. We report a case of RI that developed due to renal artery and vein thrombosis three weeks after renal cyst aspiration, as confirmed by pathological evaluation of the nephrectomy material.

CASE PRESENTATION

A 65 year-old female was admitted to the emergency care unit with complaints of colic pain over the right costovertebral region, oliguria and fever. The patient had undergone a nephrectomy due to a tumor six years earlier, and renal cyst aspiration had been performed three weeks prior to admission due to flank pain caused by the renal cyst. Her vital signs were as follows: temperature 38.5°C, blood pressure 130/90 mmHg, and pulse of 86/min. The physical examination revealed decreased turgor tonus of the skin, dry mucosal surfaces, and tenderness over the right costovertebral angle. The laboratory work-up on admission showed creatinine (Cre): 2.98 mg/dl, urea: 127 mg/dl, aspartate aminotransferase: 90 U/L, alanine aminotransferase: 41 U/L, lactate dehydrogenase (LDH): 2461 U/L, C-reactive protein (CRP): 323 mg/dl (0-5 mg/L), white blood cells (WBC): 22600 mL, neutrophil (Neu): 19900 mL, hemoglobin: 14.6 gr/dl, and hematocrit: 45%. She underwent hemodialysis because of the progressive elevation of Cre and anuria on follow-up exams. Due to grade 1 hydronephrosis that was shown on urinary system ultrasonography and the continuation of anuria, initially a double-j stent was placed. But urine output did not improve and hydronephrosis not reduced. Therefore a percutaneous nephrostomy catheter was inserted in the renal pelvis. No urine output was yielded within 10 h observation after placement of the catheter; even, although the nephrostomy catheter was in the correct position. At that point the catheters were withdrawn due to the possibility of infection. The follow-up ultrasonography showed no changes in the grade of hydronephrosis after nephrostomy catheterization. She had fever on admission, therefore vancomycine, ciprofloxacin, and meropenem were started empirically after taking urine and blood cultures. Because of the persistency of fever in spite of antibiotics and the recent history of renal cyst

Corresponding Author: Habib EMRE, Department of Nephrology, Yuzuncu Yil University, Van65100, Turkey. Tel: +90 505 9227406 Fax: +90 432 216 75 19 E-mail: habibemre@gmail.com

Abbreviations: Cre, creatinine; CRP, C-reactive protein; CT, computerized tomography; LDH, lactate dehydrogenase; MR, magnetic resonance imaging; Neu, neutrophil; RI, renal infarction; WBC, white blood cells.

aspiration, magnetic resonance imaging (MR) and diffusion MR were performed on suspicion of renal abscess. MR showed a grade 1 hydroureteronephrosis and a complicated cyst 55 mm in diameter in the middle of the right kidney. No growth was observed in the cultures of the aspiration material of the cyst. Due to the persistency of the fever despite antibiotics, and the patient's history of cyst aspiration and elevated LDH level, abdominal computerized tomography (CT) with contrast was performed in the patient on suspicion of possible RI. Abdominal CT showed a triangular hypodense area in the pericapsular region of the right kidney (Fig. 1). Because of uncontrolled infection despite all possible treatments and a worsening of her general condition, right nephrectomy was performed. The macroscopic evaluation of the nephrectomy material was consistent with RI (Fig. 2). The pathological evaluation revealed renal artery and vein thrombosis, RI and chronic pyelonephritis. The patient's clinical condition was improved dramatically after nephrectomy. The post-nephrectomy laboratory work-up, which improved as well, showed WBC: 10100 mL, Neu: 8000 mL, CRP: 22.7 mg/L, LDH: 400 U/L. The patient was discharged from the hospital and enrolled in the hemodialysis program.

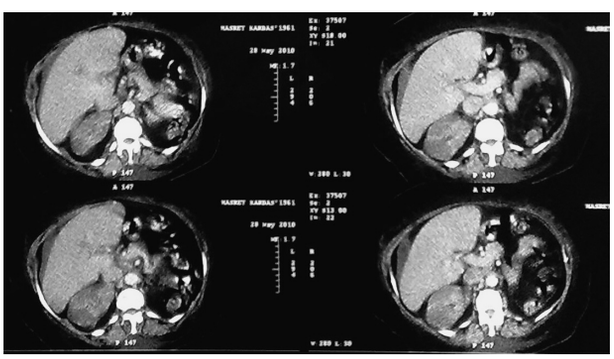

Fig. 1. Abdominal Computerized Tomography.

Fig. 2. Macroscopic Appearance of the Kidney.

DISCUSSION

RI is a rarely seen disorder. Hazanov et al. [1] reported the largest series in the literature, consisting of 44 cases. The two major causes of RI are thromboemboli, which usually originate from a thrombus in the heart or aorta, and in-situ thrombosis of a renal artery, which is less common.

The in-situ thrombosis of a renal artery may occur as a result of spontaneous or iatrogenic trauma to the renal arteries, complications of endovascular procedures, fibrodysplasia, and polyarteritis [2-4]. Renal vein thrombosis secondary to underlying systemic diseases may cause RI as well [5].

The clinical and laboratory findings of RI may mimic other commonly seen disorders including urolithiasis, pyelonephritis and acute abdomen. Thus, the detection of RI may be delayed or missed. Patients with RI usually develop severe flank pain, diffuse abdominal pain, nausea, and vomiting. Macroscopic hematuria, dysuria, fever, and less frequently oliguria can be seen in RI as well [1,2,6]. The laboratory findings in RI are non-specific. Leukocytosis, microscopic or macroscopic hematuria, leukocyturia, proteinuria, high CRP, and elevated Cre levels can be seen in RI. The most important laboratory finding is elevated LDH level. If LDH elevation is accompanied by nonspecific clinical and laboratory findings in patients with elevated risk of embolization (such as atrial fibrillation, history of recent vascular invasive procedure), RI should be considered in differential diagnosis. Further, if LDH levels are elevated to four times higher than normal with normal or mildly elevated aminotransferases, RI should be taken into account as a possible diagnosis [1,7,8].

Radiological imaging is very important in differential diagnosis. Spiral CT without contrast should be performed in a patient presenting with acute flank pain. If there is no urolithiasis and the findings are suggestive of RI, CT with contrast should be performed. The presence of a wedge shape perfusion defect in CT is highly suggestive of RI [1].

In our case, when the history, clinical presentation,

laboratory and radiological results were considered, the initial differential diagnoses were cyst infection, cyst abscess, pyelonephritis, and obstructive lesions. Due to the onset of symptoms occurring 3 weeks after cyst aspiration, no history of recent vascular procedure, and the absence of atrial fibrillation and cardiac thrombosis, the possibility of RI was not taken into account initially. After ruling out the possibility of infections and obstruction, CT with contrast was performed due to the presence of elevated LDH (2461U/L). Abdominal CT showed a triangular hypodense area in the pericapsular region of the right kidney that was consistent with RI (Fig. 1). In our case, the RI may have occurred as a result of renal artery and vein thrombosis that developed after performance of an invasive procedure (cyst aspiration) in the kidney with chronic pyelonephritis.

The normal human kidney can tolerate ischemia only 60-90 min. Prolonged ischemia, longer than three h, may cause permanent damage to the renal function [9]. Thus, early diagnosis and treatment is very important. However, the detection can be missed or delayed because of the factors that were mentioned above. The main treatments of RI are heparin infusion, thrombolytic therapy, and embolectomy. The controlling of high blood pressure and supportive treatment for renal insufficiency are very important as well [10]. If the patient has refractory hypertension, trauma-related-RI or a medically resistant situation, nephrectomy can be suggested as an alternative treatment option [11].

In our case, thrombolytic or anticoagulation therapy could not be administered because the patient applied to our clinic 3 days after onset of the symptoms. Since the infection had not been controlled despite administration of wide spectrum antibiotics, and the patient's general condition was deteriorating, the patient underwent nephrectomy. The patient's clinical and laboratory findings were improved dramatically after nephrectomy.

CONCLUSION

When a patient develops anuria, fever, and colic pain over the costovertebral angle after invasive procedures for kidney, RI should be also considered in differential diagnosis along with procedure-related complications such as bleeding and infection. An LDH level four times higher than normal accompanying these clinical symptoms could be an indication of possible RI.

REFERENCES

1. AU Hazanov N, Somin M, Attali M, Beilinson N, Thaler M et al. Acute renal embolism. Forty-four cases of renal infarction in patients with atrial fibrillation. Medicine (Baltimore) 2004; 83:292–299.
2. Paris B, Bobrie G, Rossignol P, Le Coz S, Chedid A et al. Blood pressure and renal outcomes in patients with kidney infarction and hypertension. J Hypertens 2006; 24:1649–1654.
3. Bockler D, Krauss M, Mansmann U, Halawa M, Lange R et al. Incidence of renal infarctions after endovascular AAA repair: rela tionship to infrarenal versus suprarenal fixation. J Endovasc Ther 2003; 10:1054–1060.
4. Cosby RL, Miller PD, and Schrier RW. Traumatic renal artery thrombosis. Am J Med 1986; 81:890–894.
5. Makino M, Honda H, Miyoshi F, Ban Y, Katagiri T et al. A fulminant case of renal vein thrombosis in a patient with autoimmune disorder and membranous nephropathy. Intern Med 2008; 47:969-973.
6. Robinson S, Nichols D, Macleod A, and Duncan J. Acute renal artery embolism: a case report and brief literature review. Ann Vasc Surg 2008, 22:145–147.
7. Domanovits H, Paulis M, Nikfardjam M, Meron G, Kürkciyan I et al. Acute renal infarction. Clinical characteristics of 17 patients. Medicine (Baltimore) 1999; 78:386-394.
8. Korzets Z, Plotkin E, Bernheim J, and Zissin R. The clinical spectrum of acute renal infarction. Isr Med Assoc J 2002; 4:781-784.
9. Greenberg JM, Steiner MA, and Marshall JJ. Acute renal artery thrombosis treated by percutaneous rheolytic thrombectomy. Catheter Cardiovasc Interv 2002; 56:66–68.
10. Markowitz GS, Brignol F, Burns ER, Koenigsberg M, and Folkert VW. Renal vein thrombosis treated with thrombolytic therapy: case report and brief review. Am J Kidney Dis 1995; 25:801-806.
11. Gidaro S, Schips L, and Cindolo L, Ziguener R. Laparoscopic nephrectomy for complete renal infarction due to post traumatic renal artery thrombosis. Arch Ital Urol Androl 2008; 80:79-81.

Case Report

Kurume Medical Journal, 58, 63-65, 2011

Giant Liposarcoma Occupying Most of The Hemi-Thorax and Resected in the Supine Position: Report of a Rare Case

TOSHIHIRO MATSUO, SHINZO TAKAMORI, NAOFUMI HAYABUCHI*,
MUTA FUMIHIKO, MASAKI KASHIHARA, KOUICHI YOSHIYAMA,
TATSUYA NISHI, DAIGO MURAKAMI
AND KAZUO SHIROUZU

Department of Surgery and radiology, Kurume University School of Medicine, Kurume 830-0011, Japan*
Received 11 April 2011, accepted 19 July 2011

Edited by MASAYOSHI KAGE

Summary: Liposarcoma originating in the thoracic cavity is not common. It has been reported that neither chemotherapy nor radiotherapy is effective, and that surgical resection is the only therapeutic option. There have been several cases reported of a large liposarcoma compressing adjacent organs such as the lung and the heart. In such cases, careful management is required to prevent adverse cardiopulmonary events during resection. Here we report a rare case of a 52-year-old male who had a giant liposarcoma occupying the majority of the right thorax. The patient was placed in the supine position, and the tumor was resected through an anterior thoracotomy. Percutaneous cardiopulmonary support (PCPS) was prepared in case of need. However, we succeeded in resecting the huge tumor without use of PCPS. We were unable to completely resect the tumor because it originated from the posterior mediastinum and extended into the left thorax. The resected tumor weighed 3,500 g and was 28 cm in largest diameter. The postoperative course was uneventful, except for hypoxemia lasting a few days caused by re-expansion edema in the lung. The patient was discharged and is alive at five years to date.

Key words liposarcoma, Percutareous cardiopulmonary support

INTRODUCTION

Liposarcoma arising in the thoracic cavity is rare. It has been reported that many patients have other symptoms due to the huge tumor occupying the majority of the thoracic cavity. Liposarcoma is not sensitive to chemotherapy or radiotherapy. Surgical resection is considered the only therapeutic option. When resecting a huge tumor occupying the majority of the thoracic cavity, however, care should be taken to prevent cardiopulmonary distress caused by compression of the airway, the heart, the great vessels, and other organs. Here we present a rare case of a giant liposarcoma occupying two-thirds of the right thoracic cavity, which was successfully treated with surgical resection through anterior thoracotomy.

CASE REPORT

A 52-year-old male presenting with shortness of breath was admitted to our hospital. Chest CT scan showed a huge mass and displacement of the inferior vena cava and left atrium (Fig. 1). It was diagnosed as a soft part tumor occupying two-thirds of the right thoracic cavity. We decided to resect the tumor and informed consent was obtained. In order to reduce the risk of an adverse cardiac event caused by compression of the heart and the great vessels during surgery, the patient was placed in the supine position, and the right subclavian artery and right femoral vein were isolated and taped to enable immediate use, in case of need, of percutaneous cardiopulmonary support (PCPS). Anterior thoracotomy was performed. The tumor was situated in the posterior mediastinum with a clear mar-

Corresponding author: Toshihiro Matsuo, Department of Surgery, Kurume University School of Medicine, 67 Asahi machi, Kurume 830-0011, Japan. Tel: 81+942-31-7566 Fax: 81+942-34-0709 E-mail: tomatsu@med.kurume-u.ac.jp

Abbreviations: PCPS, percutaneous cardiopulmonary support; IVC, inferior vena cava.

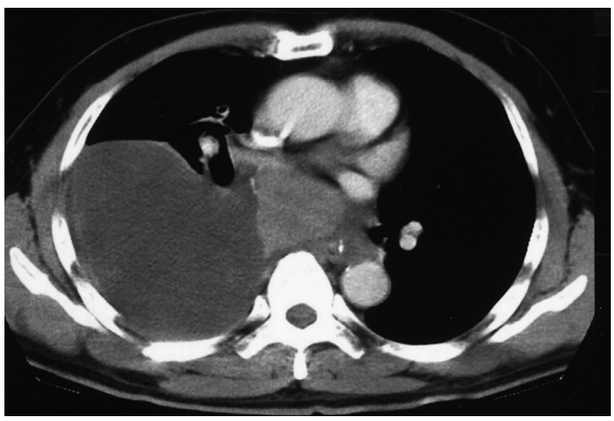

Fig. 1. Computed tomography shows a large mass with low attenuation occupying two-thirds of the right thoracic cavity, displacing the inferior vena cava and the left arterium.

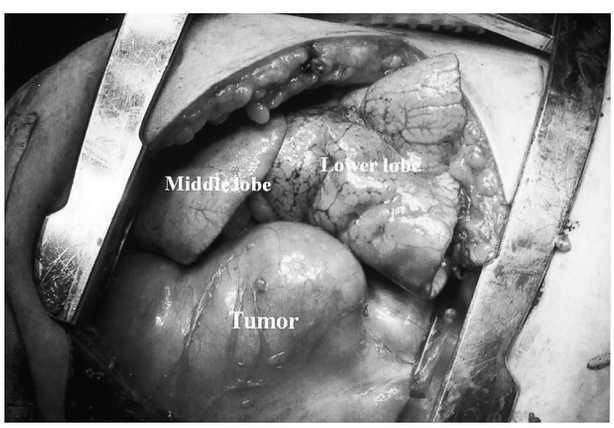

Fig. 2. Operative findings show a tumor with a well-defined margin originating in the posterior mediastinum.

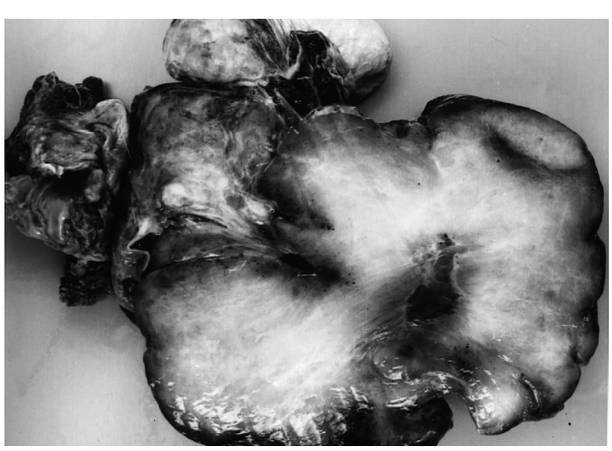

Fig. 3. The cut surface of the tumor appears to be yellowish pale and gelatinous. Focal necrosis and hemorrhage are found in the tumor.

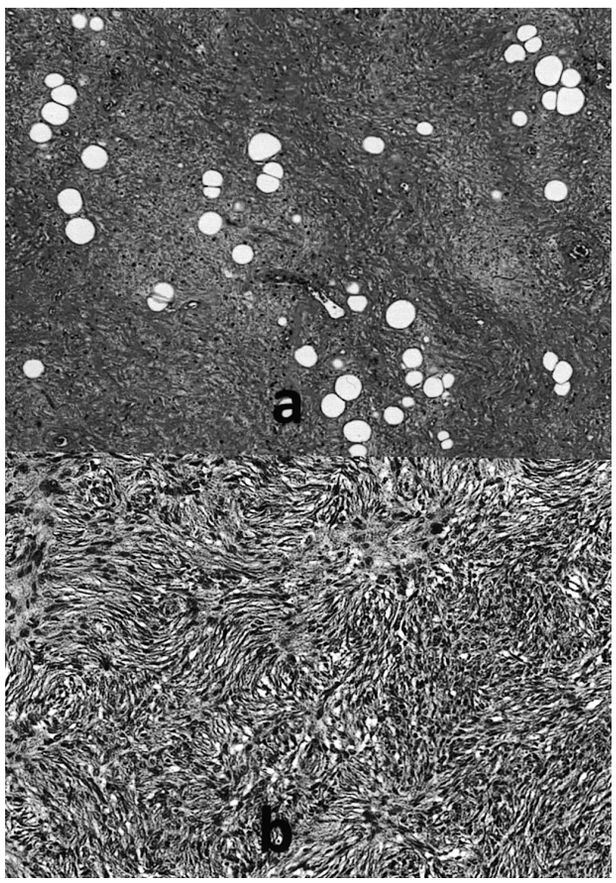

Figs. 4a and b. The tumor consists of two components. The lipogenic area is composed of mature lipocytes including lipoblasts (a: H.E. stain x40). The nonlipogenic area is composed of proliferation of atypical spindle or mildly pleomorphic cells arranged in a storiform pattern (b: H.E. stain ×100).

gin covered by the pleura. However, it was not encapsulated (Fig. 2). Although the majority of the tumor was resected through the right thoracic cavity, a small portion extending into the left thoracic cavity could not be removed. No cardiac event occurred. The excised tumor weighed 3500 g and was 28 cm in large diameter. The cut surface of the tumor had a pale yellowish gelatinous appearance (Fig. 3) and was composed of fat cells, including lipoblasts embedded in an abundant fibrocollagenous or focally myxoid stroma including atypical spindle cells (Figs. 4 a and b). Immunohistochemically, the spindle cells in the dedifferentiated area were positive for alpha-smooth muscle actin and focally for h-caldesmon, suggesting myofibroblastic differentiation, whereas muscle specific actin (HHF35), desmin, S-100, CD34, bcl-2, cytokeratins (CAM5.2, AE1/AE3) and EMA were negative. It was histologically diagnosed as dedifferentiated liposarcoma. After surgery the patient experienced slight

hypoxemia caused by re-expansion pulmonary edema, which improved within a few days. The patient was discharged on the 46th POD. Ten months later the patient received heavy-ion radiotherapy for the residual mass. The patient is alive at four years to date.

DISCUSSION

Liposarcoma is a soft-part sarcoma [1]. However, liposarcoma originating in the thoracic cavity is not common. Among patients with liposarcoma in the thoracic cavity, 85% have related symptoms, while 15% have no symptoms and the tumor is generally discovered on routine chest radiography [2].

Klimstra et al. [3] reported that the average tumor size was 15.7 cm, ranging from 6 to 40 cm, and the average tumor weight was 1500 g. Such a huge tumor commonly compresses the intra-thoracic organs such as the lung, the heart, great vessels and others, and occasionally causes life-threatening conditions. Complete surgical excision is the first choice of treatment [4]. No effect by induction or adjuvant chemotherapy for liposarcoma has been shown. Radiotherapy also appears to be ineffective for such tumors. The life-threatening conditions caused by a huge tumor compressing the lung and the heart can be resolved only by surgical excision of the tumor. To prevent serious adverse events caused by compression of the heart and the great vessels, however, careful management is required during surgery. We decided against a lateral incision in the lateral decubitus position, and chose an anterior thoracotomy in the supine position. Moreover, we prepared PCPS, in case of need, to deal with any cardiopulmonary emergency during surgery.

Ohta et al. [5] reported a patient who underwent resection of recurrent mediastinal liposarcoma through a clamshell approach and suggested that such aggressive surgery could improve the quality of life and prolong the survival of the patient. In the present case, complete resection of the tumor was not achieved, because it occupied the posterior mediastinum and extended into the left thoracic cavity. Grewal et al. [6] reported a 75-year-old patient who survived more than five years after incomplete resection of an uncapsulated liposarcoma in the anterior mediastinum followed by radiotherapy. There remains some controversy over adjuvant therapy, in particular radiotherapy, for liposarcoma because of doubts about efficacy, and the later difficulty for surgery if any recurrence has to be resected.

We have reported a rare case of surgical resection of a huge liposarcoma occupying most of the hemithoracic cavity. The resected tumor weighed 3,500 g and was 28 cm in largest diameter. We concluded in the present case that surgery was effective in reducing the risk to cardiopulmonary distress, even though resection was incomplete. In case of surgical resection of a huge tumor in the thoracic cavity, careful perioperative management is important and preparations should be made to cope with any adverse cardiopulmonary event that might occur during surgery.

REFERENCES

1. Enzinger FM, and Weiss SW. Soft Tissue Tumor. St Lois: CV Mosby; 1995, p.431.
2. Schweitzer DL, and Aguam AS. Primary liposarcoma of the mediastinum. Report of a case and review of the literature. J Thorac Cardiovasc Surg 1977; 74:83-97.
3. Klimstra DS, Moran CA, Perino G, Koss MN, and Rosai J. Liposarcoma of the anterior mediastinum and thymus: a clinicopathologic study of 28 cases. Am J Surg Pathol 1995; 19:782-791.
4. Peng C, Zhao X, Dong X, and Jiang X. Liposarcoma of the pleural cavity: a case report. J Thorac Cardiovasc Surg 2007; 133:1108-1109.
5. Ohta Y, Murata T, Tamura M, Sato H, Kurumaya H et al. Surgical resection of recurrent bilateral mediastinal liposarcoma through the clamshell approach. Ann Thorac Surg 2004; 77:1837-1839.
6. Grewal RG, Prager K, Austin JH, and Rotterdam H. Long-term survival in non-encapsulated primary liposarcoma of the mediastinum. Thorax 1993; 48:1276-1277.

Case Report

Kurume Medical Journal, 58, 67-72, 2011

Giant Malignant Phyllodes Tumor: A Case Report

MIKI TAKENAKA*,**, UHI TOH**, HIROKO OTSUKA**, HIROKI TAKAHASHI**, NOBUTAKA IWAKUMA**, SHINO NAKAGAWA**, TERUHIKO FUJII**, RIN YAMAGUCHI*, HIROHISA YANO*, KAZUO SHIROUZU** AND MASAYOSHI KAGE†,‡

Department of Pathology and Surgery**, Kurume University School of Medicine,*
†Department of Diagnostic pathology, Kurume University Hospital,
‡Research Center for Innovative CancerTherapy, Kurume University, Kurume 830-0011, Japan

Received 8 June2011, accepted 1 September 2011

Summary: We present a case of a 57-year-old woman with a giant malignant phyllodes tumor (PT) in her right breast, with maximum diameter of 20 cm. The core-needle and excisional biopsy specimens were diagnosed as suspicious for low-grade myofibroblastic sarcoma (LGMS). The subsequent total mastectomy with partial resection of the pectoral muscles showed predominance of stromal hypercellularity without an epithelial component. However, we diagnosed this as a malignant PT because focal areas showed a leaf-like pattern. In the case of large malignant PTs that exhibit stromal predominance, it can be difficult to distinguish between a pure sarcoma and malignant PT. It is important to thoroughly examine multiple sections from the view point of residual epithelial structure in morphological diagnosis.

Key words giant phyllodes tumor, phyllodes tumor, phyllodes tumor malignant type

INTRODUCTION

Phyllodes tumor (PT) of the breast is a rare biphasic fibroepithelial neoplasm that accounts for less than 1% [1] of primary breast neoplasms. PT usually presents as a rapidly growing and clinically benign breast lump in females within the fourth or fifth decade of life [2,3]. PT typically exhibits an enhanced intracanalicular growth pattern with leaf-like projections into dilated lumens. Malignant PTs are more readily characterized by stromal pleomorphism and overgrowth, frequent mitoses and infiltrative borders [4]. In case of large growing malignant PTs with stromal predominance, it is difficult to distinguish between a pure sarcoma and malignant PT. We discuss herein recent advances in the diagnosis and management of PT.

CASE REPORT

A 57-year-old woman presented with a 20- year history of swelling of the right breast. She was referred to another hospital due to a painful and swollen right breast with bleeding. Physical examination revealed a massively enlarged right breast over 20 cm in maximum diameter. Core-needle biopsy was suspicious for low-grade myofibroblastic sarcoma (LGMS). She was transferred to our hospital for further treatment.

Her only significant past medical history was a duodenal ulcer. She had no history of pregnancy or nursing and her family history was unremarkable. Laboratory data were as follows: red blood cell count, $247\times10^4/\mu l$; hemoglobin, 6.9 g/dl; albumin, 1.55 g/dl and C-reactive protein, 11.8 mg/dl. She exhibited severe anemia, hypoalbuminemia and systemic inflammation. Tumor markers including CEA and CA15-3 were within normal limits.

Physical examination showed a giant tumor of the right breast, with ulceration, exudate, bleeding, and foul smell (Figs. 1). She could not move her right arm due to the severe pain.

Corresponding author: Miki Takenaka Department of Pathology, Kurume University School of medicine 67 Asahi-machi, Kurume city, Fukuoka 830-0011, Japan. Tel: +81-942-31-7546 Fax: +81-942-0905 E-mail: takenaka_miki@kurume-u.ac.jp

Abbreviations: PT, phyllodes tumor; LGMS, low-grade myofibroblastic sarcoma; CT, computed tomography; MRI, magnetic resonance imaging; HE, hematoxylin and eosin.

a b

Figs. 1 (a,b). Grossly enlarged patient's right breast with ulceration, exudate, bleeding and foul smell.

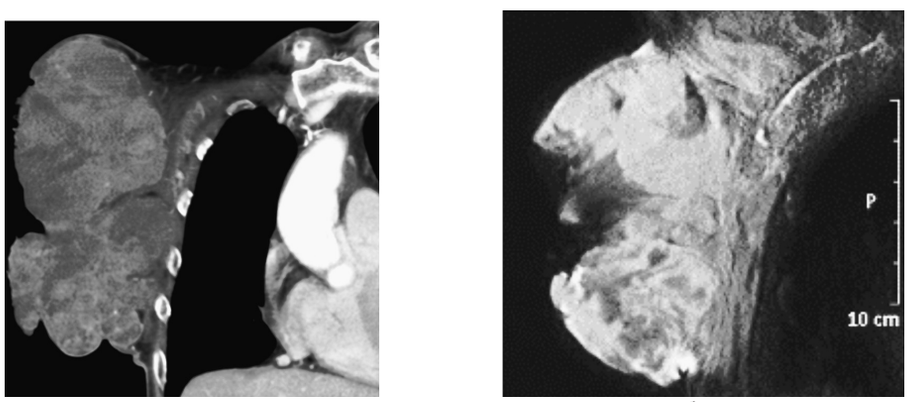

a b

Figs. 2 (a,b). a. CT shows a 20×14×9.7 cm heterogenously enhanced mass that is suspicious for the chest wall invasion. b. T2 weighted MRI shows heterogenous pattern with high signal intensity.

Mammographic and ultrasonographic examinations could not be carried out because of the pain caused by the huge tumor. Computed tomography (CT) showed a 20×14×9.7 cm heterogenous breast mass with diffuse enhancement that was suspicious for chest wall invasion (Fig. 2a). T2 weighted magnetic resonance imaging (MRI) study revealed a heterogenous pattern with high signal intensity (Fig. 2b). Axillary lymph nodes were not detected in MRI.

We performed an excisional biopsy of the tumor, which showed marked stromal hypercellularity without an epithelial component. By immunohistochemistry staining, the stromal cells were positive diffusely for alpha smooth muscle actin, Calponin, HHF35, CD10 and vimentin. But they were negative for desmin, S-100, CD34, epithelial membrane antigen and AE1/AE3. Reactivity with MIB-1 and p53 was seen in 20.6% and 24.7% of the cells, respectively. Histopathological diagnosis of the excisional specimen was the same as the prior core-needle biopsy: "suspicious for LGMS" .

Her hemoglobin improved from 6.9 g/dl to 11.0 g/dl by preoperative blood transfusion. Furthermore we performed transcatheter arterial embolization of the breast tumor in order to reduce blood loss during the operation and applied Mohs' paste, which is often used for hemorrhagic tumors to reduce the amount of exudate, bleeding and foul smell. Administration of internal oxycodone hydrochlorides relieved the severe breast pain.

She underwent a modified radical mastectomy with sufficient surgical margin, and partial resection of the pectoral muscles. The tumor had no invasion into the rib, but axillary lymph nodes were swollen. The wound was able to close primarily, without skin grafting (Figs. 3), and the total blood loss was 985 cc.

The resected tumor specimen measured 21.5×16×9 cm and weighed 2120 g, and appeared as a white, soft and mucoid homogenous mass with focal hemorrhage. Microscopic findings showed a highly cellular stromal tumor composed of spindled cells with marked atypia and brisk mitotic activity (mean: 30/10HPFs) (Figs 4a,b). Immunohistochemically, MIB-1 and p53 was seen in 50.5% and 41.3% of the cells, respectively

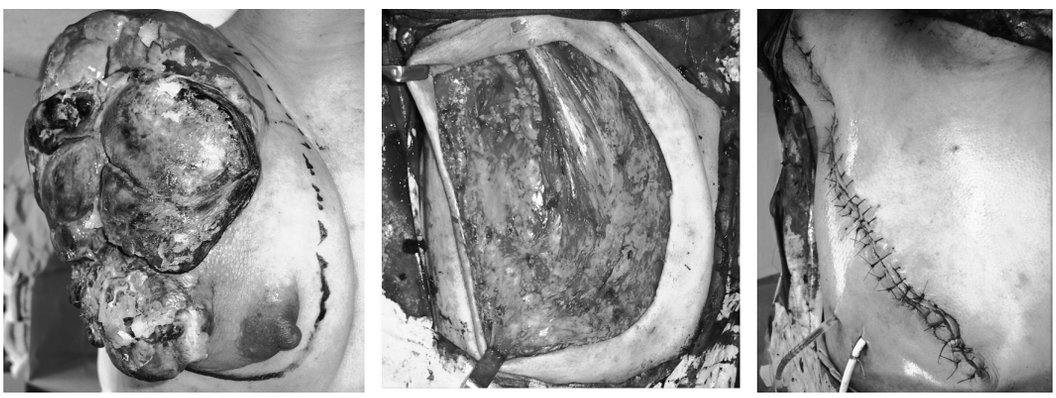

a b c

Figs. 3(a,b,c). Operative findings: A modified radical mastectomy and partial resection of pectoral muscles were performed.

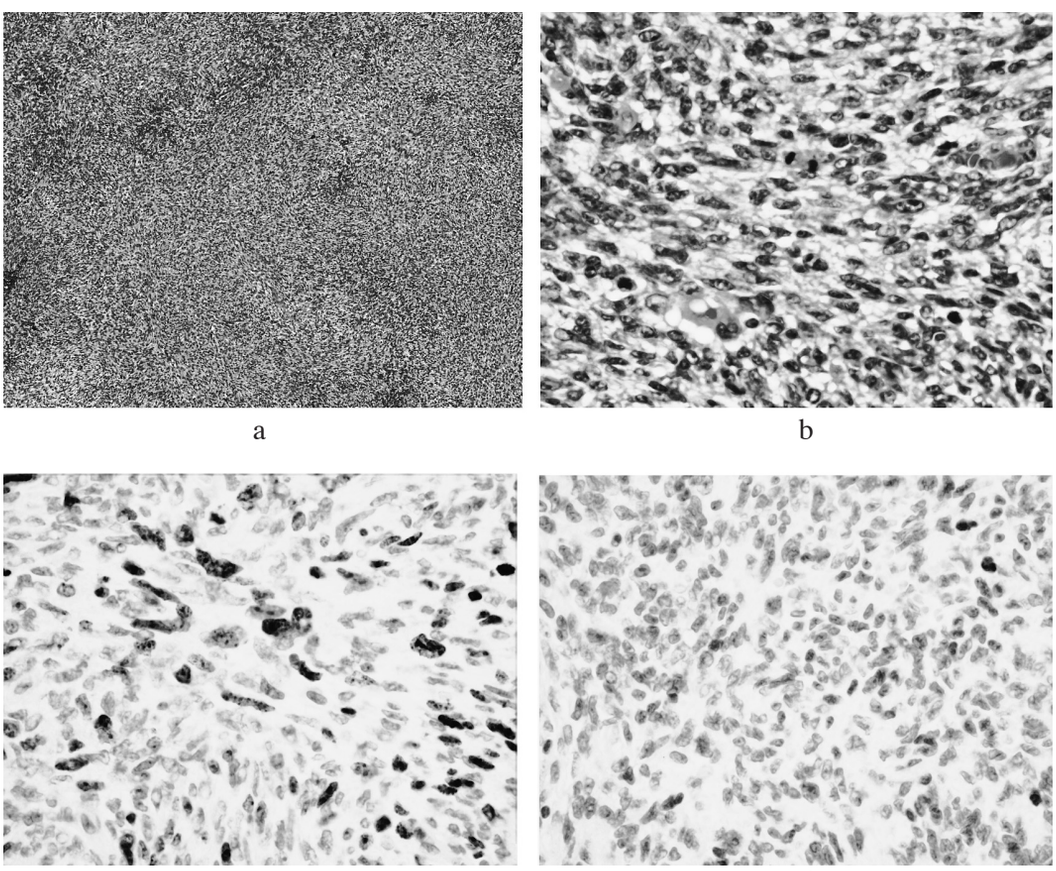

a b

c d

Figs. 4(a,b,c,d). Histopathological findings: The tumor is highly cellular with stromal overgrowth. They are spindled in shape with marked atypia and brisk mitotic activity (HE stain, a: ×100, b: ×400 magnification). Immunohistochemically, MIB-1(c) and p53 (d) was seen in 50.5% and 41.3% of the cells, respectively (c, d: ×400 magnification).

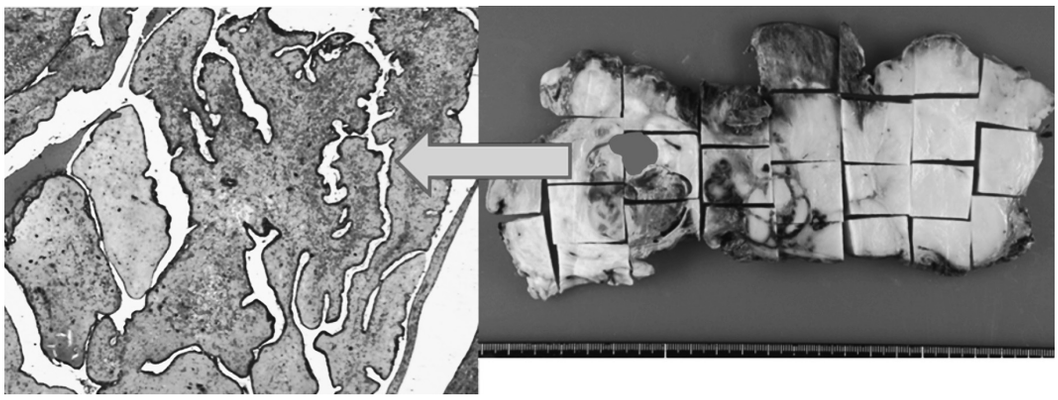

a b

Figs. 5(a,b). Histopathological findings by multiple sections: There is an epithelial component with leaf-like pattern appeared in the tumor (a: HE stain, ×40 magnification).

(Figs. 4c,d). Some stromal cells showed lipoblast-like differentiation. However, further careful examination of additional sections revealed an epithelial component with a leaf-like pattern (Figs. 5). The final histopathological diagnosis was PT, malignant type. The margin of the resected tumor showed partially infiltrative growth into skin, but no invasion into muscles or lymphovasa. There were no axillary lymph node metastases.

She recovered well, and there was no evidence of local recurrence or distant metastasis 17 months after surgery without adjuvant chemotherapy.

DISCUSSION

PT of the breast is a rare biphasic fibroepithelial neoplasm that accounts for about 1% [1] of primary breast tumors. The disease occurs predominantly in middle-aged women, with the average age of presentation at 40 years old [5-8]. They often present clinically as a painless mass with an average size of 4-5 cm [9,10]. The first treatment of choice is surgical resection. Axillary lymph node metastasis is rare, and lymph node dissection is not required. The role of adjuvant therapy for PT with chemotherapy and/or radiation therapy has not been clearly defined by prospective studies [6,11].

Although local recurrence is common (21% for benign types, 46% for borderline types, and 65% for malignant types [12]), prognosis is generally good, with 5-year survival rates of 91% and 82% for benign/borderline types and malignant type [2], respectively. Local recurrence has been associated with a positive surgical margin, stromal overgrowth and histological classification. Stromal overgrowth was an especially predictive factor for local recurrence in cases with a positive surgical margin [13].

Many biological markers have been evaluated for their prognostic value, and cell proliferation has shown a correlation between MIB-1 positivity and histologi-

TABLE 1.
Immunohistochemical staining results

Material	AE1/AE3	Vimentin	α-SMA	Calponin	HHP35	CD10	MIB-1	p53
Biopsy	−	+ (weak)	+	+	+	+	20.6%	24.7%
Resected specimen The stroma of hypercellularity	−	++	++	−	++	+	50.5%	41.3%
Resected specimen The stroma of leaf-like pattern	−	++	+	−	+	+ (focal)	8.6%	14.2%

cal grade. Expression of p53, commonly used as a surrogate for identification of a tumor suppressor gene mutation, has been correlated with tumor grade. Among biological markers, MIB-1 index (0.7-6% for benign types, 11.2% for borderline types and 30-31.2% for malignant types [14,15]) and p53 expression status (0-4% for benign/borderline types and 55-56% for malignant types [8,14]) may be significant prognostic factors. Table 1 summarizes immunohistochemical staining results of this case.

The tumor size and several US and MRI findings can be used to help preoperatively distinguish between malignant or benign PT. In MRI, internal non-enhanced septations, silt-like patterns in enhanced images and signal changes from T2-weighted to enhanced images correlated significantly with the histologic grade [16]. In this case, MRI findings were not characteristic of PT.

PT typically exhibits an enhanced intracanalicular growth pattern with leaf-like projections into dilated lumens. In the malignant types, the stroma shows frank sarcomatous changes, which most often are fibrosarcoma-like. Due to overgrowth of the sarcomatous components, the epithelial component may only be identified after examining multiple sections. As malignant PT grows larger and the stromal component predominates, it becomes difficult to distinguish between pure sarcoma and malignant PT.

LGMS seems to represent a distinct entity in the spectrum of low-grade myofibroblastic neoplasms and is distinguishable from fibromatosis, myofibromatosis, solitary fibrous tumor, fibrosarcoma, and leiomyosarcoma [17]. LGMS of the breast is very rare, and only seven cases have been reported in the literature [18].

The final diagnosis differed from the biopsy diagnoses due to the focal presence of an epithelial component in the resected specimen. In case of biopsy specimens showing predominately stromal lesions, it is important to thoroughly examine the resected specimen for possible epithelial components.

In conclusion, diagnosis of PT, and assignment of histological characteristics are still fraught with uncertainties, but the method described here is probably still the most practical approach [19]. Assessment of biological markers does not significantly improve prognostic prediction. Further molecular level assessment of PT may provide more insight into the biology of this tumor.

REFERENCES

1. El Khouli RH, and Louie A. Case of the season: a giant fibroadenoma in the guise of a phyllodes tumor; characterization role of MRI. Semin Roentgenol 2009; 44:64-66.
2. Chaney AW, Pollack A, McNeese MD, Zagars GK, Pisters PW et al. Primary treatment of cystosarcoma phyllodes of the breast. Cancer 2000; 89(7):1502-1511.
3. Korpanty G, Power DG, Murphy C, Kell M, and McCaffery J. Phyllodes tumor of the breast. Med Oncol.
4. Lee, A.H., Recent developments in the histological diagnosis of spindle cell carcinoma, fibromatosis and phyllodes tumour of the breast. Histopathology 2008; 52(1):45-57.
5. Barrio AV, Clark BD, Goldberg JI, Hoque LW, Bernik SF, et al. Clinicopathologic features and long-term outcomes of 293 phyllodes tumors of the breast. Ann Surg Oncol 2007; 14(10):2961-2970.
6. Belkacemi Y, Bousquet G, Marsiglia H, Ray-Coquard I, Magne N et al. Phyllodes tumor of the breast. Int J Radiat Oncol Biol Phys 2008; 70(2):492-500.
7. Ben Hassouna J, Damak T, Gamoudi A, Chargui R, Khomsi F et al. Phyllodes tumors of the breast: a case series of 106 patients. Am J Surg 2006; 192(2):141-147.
8. Chen WH, Cheng SP, Tzen CY, Yang TL, Jeng KS et al. Surgical treatment of phyllodes tumors of the breast: retrospective review of 172 cases, in J Surg Oncol 2005; 91:185-194.
9. Bellocq J and Margo G. Fibroepithelial tumors. In:Tavassoli FA, Devilee P, editors. World Health Organization Classification of Tumors. Pathology and Genetics of the Breast and Female Genital Organs Lyon: IARC press, 2003:100-103.
10. Rosen, P., Fibroepithelial Neoplasms. In: Rosen PP, editor. Rosen's Breast Pathology New York: Lippincott-Raven, 1997:155-173.
11. Morales-Vasquez F, Gonzalez-Angulo AM, Broglio K, Lopez-Basave HN, Gallardo D et al. Adjuvant chemotherapy with doxorubicin and dacarbazine has no effect in recurrence-free survival of malignant phyllodes tumors of the breast. Breast J 2007; 13(6):551-556.
12. Barth RJ Jr. Histologic features predict local recurrence after breast conserving therapy of phyllodes tumors. Breast Cancer Res Treat 1999; 57(3):291-295.
13. Taira N, Takabatake D, Aogi K, Ohsumi S, Takashima S et al. Phyllodes tumor of the breast: stromal overgrowth and histological classification are useful prognosis-predictive factors for local recurrence in patients with a positive surgical margin. Jpn J Clin Oncol 2007; 37(10):730-736.
14. Erhan Y, Zekioglu O, Ersoy O, Tugan D, Aydede H et al. p53 and Ki-67 expression as prognostic factors in cystosarcoma phyllodes. Breast J 2002; 8(1):38-44.
15. Yonemori K, Hasegawa T, Shimizu C, Shibata T, Matsumoto K et al. Correlation of p53 and MIB-1 expression with both the systemic recurrence and survival in cases of phyllodes tumors of the breast. Pathol Res Pract 2006; 202(10):705-712.
16. Tan H, Zhang S, Liu H, Peng W, Li R, Gu Y et al. Imaging findings in phyllodes tumors of the breast. Eur J Radiol 2011(in press).
17. Mentzel T, Dry S, Katenkamp D and Fletcher CD. Low-grade myofibroblastic sarcoma: analysis of 18 cases in the spectrum of myofibroblastic tumors. Am J Surg Pathol 1998; 22(10):1228-1238.

18. Morgan PB, Chundru S, Hatch SS, Hawkins HK, Adegboyega PA et al. Uncommon malignancies: case 1. Low-grade myofibroblastic sarcoma of the breast. J Clin Oncol 2005; 23(25):6249-6251.
19. Tse GMK, Niu Y, and Shi HJ. Phyllodes tumor of the breast: an update. Breast Cancer 2010; 17(1):29-34.